WIND
ENERGY
SCIENCE

eawe
european academy of wind energy

Probabilistic cost modeling as a basis for optimizing inspection and maintenance of turbine support structures in offshore wind farms

Muhammad Farhan[1]**, Ronald Schneider**[1]**, Sebastian Thöns**[1,2]**, and Max Gündel**[3]

[1]Bundesanstalt für Materialforschung und -prüfung (BAM), Berlin, Germany
[2]Division of Structural Engineering, Lund University, Lund, Sweden
[3]Chair of Steel Construction, Helmut-Schmidt-Universität/
Universität der Bundeswehr Hamburg, Hamburg, Germany

Correspondence: Muhammad Farhan (muhammad.farhan@bam.de)

Abstract. The operational management of offshore wind farms includes inspection and maintenance (I&M) of the wind turbine support structures. These activities are complex and influenced by numerous uncertain factors that affect their costs. The uncertainty in the I&M costs should be considered in decision value analyses performed to optimize I&M strategies for the turbine support structures. In this paper, we formulate a probabilistic parametric model to describe I&M costs for the common case in which a wind farm is serviced and maintained using a workboat-based strategy. The model is developed based on (a) interviews with a wind farm operator, engineering consultants, and operation and maintenance engineers, as well as (b) scientific literature. Our methodology involves deriving the probabilistic models of the cost model parameters based on intervals representing a subjective expert opinion on the foreseeable ranges of the parameter values. The probabilistic cost model is applied to evaluate the total I&M costs, and a sensitivity analysis is conducted to identify the main cost drivers. The model can be utilized to optimize I&M strategies at the component, structural system, and wind farm level. To illustrate its potential use, we apply it in a numerical study in which we optimize I&M strategies at the structural system level and identify and demonstrate a simplified approach of capturing uncertain I&M costs in the optimization. The simplified approach is generalized and made available for maintenance cost optimization of offshore wind turbine structures.

1 Introduction

The harsh offshore environment in combination with the rotor dynamics affects the condition and integrity of the wind turbine (WT) support structures in offshore wind farms. To improve the condition of deteriorated structural components and, consequently, to prevent failures of the WT support structures, wind farm operators perform condition-based or possibly predictive maintenance. Maintenance is classified as condition-based when scheduled based on the current component or system condition which is inferred from inspection and monitoring outcomes and predictive when carried out based on the predicted component or system condition

where the model-based predictions are informed by the available inspection and monitoring outcomes and the previously performed maintenance actions.

Wind farm operators typically conduct separate inspection and maintenance (I&M) campaigns to first collect information on the condition of the deteriorating WT support structures and to subsequently improve it if necessary. Within this context, an inspection campaign is characterized by the campaign time and inspection method, the number of inspected WT support structures, and the number and location of the inspected components in a WT support structure. In the case that the wind farm is serviced by boats operating from a port base, an inspection campaign is additionally influenced by

the distance from the port to the wind farm, the choice of vessel, the number of personnel, the required equipment, the mobilization and demobilization activities, and the time to complete an inspection work package. Like inspection campaigns, a maintenance campaign is characterized by the campaign time and maintenance method. In addition, a maintenance campaign is influenced by the component location, the time to complete a maintenance intervention on site, the required equipment, preparations and materials, the distance between the port and the wind farm, the choice of vessel, the number of personnel, and the effort involved in engineering a maintenance intervention (i.e., designing and testing of a maintenance solution).

Clearly, I&M of deteriorating WT support structures in an offshore wind farm is associated with costs, and the total lifetime I&M costs depend on the adopted I&M strategy, which determines the time and scope of each I&M campaign based on the available system information. Condition-based and predictive maintenance strategies can be optimized at the beginning of the planned and/or extended lifetime of an offshore wind farm and adapted during its (extended) lifetime using pre-posterior analysis from Bayesian decision theory (e.g., Sorensen, 2009; Nielsen and Sorensen, 2011; Florian and Sorensen, 2017; Farhan et al., 2021; Bismut and Straub, 2021). In such an analysis, probabilistic models of (a) the governing deterioration processes including the effect of maintenance, (b) the structural performance, and (c) the inspection and monitoring performance are employed to predict the following:

- the condition of the structural components, inspection and monitoring outcomes, and maintenance actions and

- the structural component and system reliability conditional on the predicted component condition, inspection and monitoring outcomes, and maintenance actions.

In addition, a cost model is utilized to quantify the costs of inspections and monitoring as well as maintenance and the monetized consequences of structural failures. Based on these models, the expected lifetime I&M costs and the lifetime risk of structural failure can be estimated for a given I&M strategy. A cost and risk optimal I&M strategy then balances the expected lifetime I&M costs with the lifetime risk of structural failure.

In the existing literature, normalized cost ratios or deterministic cost models are utilized as a basis for optimizing I&M of deteriorating structural systems using decision-theoretical approaches (e.g., Schneider et al., 2018; Bismut and Straub, 2021; Morato et al., 2023). Although deterministic cost models enable an optimization of I&M activities, they lack the ability to capture the effect of the I&M cost uncertainties in the decision analysis, especially in applications in which I&M costs are included in the underlying models on a nonlinear basis. Importantly, probabilistic parametric cost modeling facilitates sensitivity analyses (beyond local

derivative-based sensitivity analyses) to understand the effect of the various uncertain cost-affecting factors on the total I&M costs. With regards to optimizing I&M of WT support structures in offshore wind farms, comprehensive and explicit consideration of probabilistic I&M costs in the decision analysis is – to the best of the authors' knowledge – something which has not been explored previously. In addition, this issue is also relevant, since – from our experience – wind farm operators commonly highlight the need to consider the uncertainties in the I&M costs in the optimization of I&M strategies.

Motivated by this, we develop a probabilistic parametric cost model of I&M of WT support structures in offshore wind farms. In particular, we focus on wind farms which are serviced and maintained using a workboat-based strategy, where the workboats operate from a port base. The cost model is derived based on interviews with a wind farm operator, engineering consultants, and operation and maintenance engineers, as well as scientific literature. Subsequently, we employ the model to (a) quantify the uncertainties in the total I&M costs and (b) perform a variance-based sensitivity analysis to better understand the key cost drivers. The model can be applied to optimize I&M at the component, structural system, and wind farm level. To demonstrate a potential application, we apply the cost model in a cost- and risk-informed decision value analysis to optimize I&M strategy for a steel frame subject to fatigue.

The paper is organized as follows: Sect. 2 presents a generic decision-theoretical framework, which forms the basis for optimizing I&M of WT support structures in offshore wind farms. The presentation of the material follows our previous work (Farhan et al., 2021). However, compared to our previous work, our current contribution explicitly considers the uncertainties in the I&M costs in the decision analysis. In Sect. 3, different types of I&M methods for support structures in offshore wind farms are discussed. Subsequently, different uncertain parameters are identified that influence the overall costs of an I&M strategy. Furthermore, ranges of these parameters are also presented, as estimated based on expert knowledge. To quantify the overall cost of the considered I&M activities, a deterministic cost model is first formulated in Sect. 4.1. Subsequently, in Sect. 4.2 a probabilistic I&M model is constructed by combining the deterministic cost model with a probabilistic model of its uncertain parameters. Section 5 presents the uncertainty quantification and sensitivity analysis. Section 6 summarizes the numerical example. A summary and concluding remarks are provided at the end of the paper in Sect. 7.

2   Utility-informed optimization of I&M of turbine support structures in offshore wind farms considering probabilistic I&M costs

2.1   Decision analysis

The identification of an optimal I&M strategy for turbine support structures in offshore wind farms is a decision problem under uncertainty and risk (Farhan et al., 2021). This type of problem can be solved based on Bayesian decision theory (Raiffa and Schlaifer, 1961) and graphically represented by the generic decision tree shown in Fig. 1. Each branch of the decision tree corresponds to a realization of decisions represented by square nodes and random events or random variables represented by circular nodes. As an example, the lower branch in the decision tree in Fig. 1 corresponds to a realization of (a) a decision i concerning the inspection and monitoring regime, (b) the corresponding probabilistic inspection and monitoring outcomes Z_i, (c) the decisions a concerning the maintenance actions, (d) the probabilistic parameters Y influencing the effect of the maintenance actions a, (e) the probabilistic parameters X influencing the system state, and (f) the probabilistic parameters W influencing the utility. Each of these realizations is associated with a utility U and an index representing the analysis type, depicted by the diamond-shaped leaves of the decision tree. According to utility theory (Von Neumann and Morgenstern, 1947), the maximization of the expected value of the utility U quantifies the optimality of decisions. From this it follows that the optimal decisions concerning inspection and monitoring as well as maintenance can be determined by maximizing the expected utility.

The utility U_0 associated with the upper branch of the decision tree can be described by the following generic utility function:

$$U_0(X, W) = B(X, W) - C_F(X, W), \tag{1}$$

where $B(X, W)$ and $C_F(X, W)$ describe the lifetime economic benefits from operating the wind farm and lifetime costs of structural failures as a function of X and W. Based on the utility function $U_0(X, W)$ and the prior probability distributions of X and W, the expected utility $\mathbb{E}[U_0]$ can be computed as described in Appendix A1. This quantity is primarily required as a reference value in the decision value analysis presented below in Sect. 2.2. In the literature, the evaluation of $\mathbb{E}[U_0]$ is referred to as system state analysis (SS-A) (Thöns and Kapoor, 2019).

Next, the utility U_1 associated with the center branch of the decision tree can be generically expressed by the following utility function:

$$U_1(a, Y, X, W) = B(a, Y, X, W) - C_M(a, Y, X, W) \\ - C_F(a, Y, X, W), \tag{2}$$

where $B(a, Y, X, W)$, $C_M(a, Y, X, W)$, and $C_F(a, Y, X, W)$ are the lifetime economic benefits, maintenance costs, and

failure costs as a function of a, Y, X, and W. The optimal maintenance actions a^* are identified by maximizing the conditional expected utility $\mathbb{E}[U_1|a]$, which is computed based on the utility function $U_1(a, Y, X, W)$ and the prior probability distributions of Y, X, and W, as outlined in Appendix A2. Identifying a^* in this way (i.e., without considering inspection and monitoring to inform decisions on maintenance actions) is referred to as prior decision analysis (Raiffa and Schlaifer, 1961) or predicted action decision analysis (PA-DA) (see also Thöns and Kapoor, 2019).

Finally, the utility U_2 associated with the lower branch of the decision tree can be generically written as (see also Sorensen, 2009)

$$U_2(i, Z_i, a, Y, X, W) = B(i, Z_i, a, Y, X, W) \\ - C_{SHM}(i, Z_i, a, Y, X, W) - C_I(i, Z_i, a, Y, X, W) \\ - C_M(i, Z_i, a, Y, X, W) - C_F(i, Z_i, a, Y, X, W), \tag{3}$$

where $B(i, Z_i, a, Y, X, W)$, $C_{SHM}(i, Z_i, a, Y, X, W)$, $C_I(i, Z_i, a, Y, X, W)$, $C_M(i, Z_i, a, Y, X, W)$, and $C_F(i, Z_i, a, Y, X, W)$ are the lifetime economic benefits, monitoring costs, inspection costs, maintenance costs, and failure costs as a function of i, Z_i, a, Y, X, and W. The optimal information acquisition regime (or inspection and monitoring regime) i^* is determined by maximizing the conditional expected utility $\mathbb{E}[U_2|i]$, which is determined based on $U_2(i, Z_i, a, Y, X, W)$ and the probabilistic models of Z_i, Y, X, and W as detailed in Appendix A3. As discussed in Appendix A3, this maximization jointly optimizes decisions on inspection and monitoring as well as maintenance actions based on (a) predicted information on the system condition and performance, (b) predicted maintenance actions, and (c) corresponding benefits and costs. This analysis is referred to as pre-posterior decision analysis (Raiffa and Schlaifer, 1961) or predicted information and predicted action decision analysis (PIPA-DA) (see also Thöns and Kapoor, 2019).

From Eqs. (2) and (3) it can be seen that a model for quantifying the inspection and monitoring as well as maintenance costs is a key component of the utility functions required to measure the optimality of decisions concerning I&M of WT support structures in offshore wind farms. Such a cost model should be formulated as a function of the uncertain parameters influencing the I&M costs in order to capture the uncertainties in these costs in the decision-making.

2.2   Decision value analysis

The root node in the decision tree in Fig. 1 represents the basic decision concerning the implementation of an integrity management strategy (Thöns, 2018). This decision can be informed by a decision value (DV) analysis. Following Thöns and Kapoor (2019), three different DVs may be formulated based on the decision tree shown in Fig. 1. The first DV, $V_{PA-DA}^{PIPA-DA}$, is defined as the difference between the maximum expected utility resulting from the PIPA-DA, $\mathbb{E}[U_2|i^*]$,
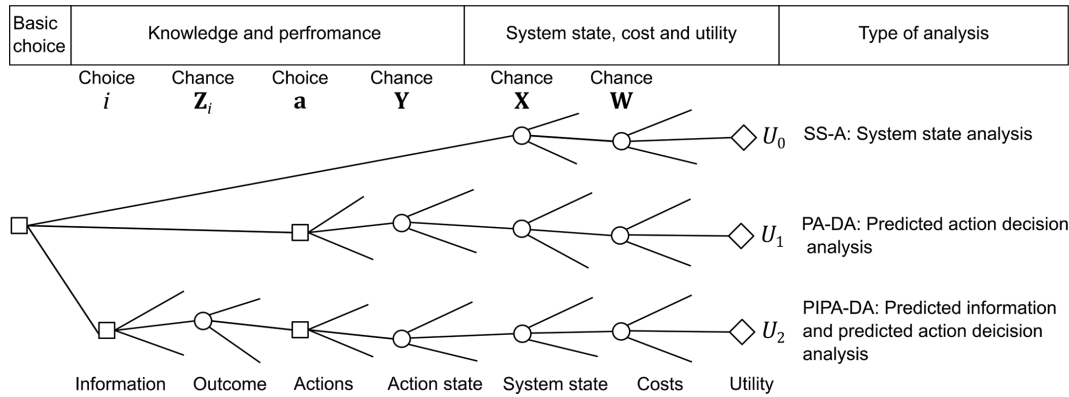
Figure 1. Generic decision tree for modeling decisions on inspection and monitoring as well as maintenance of turbine support structures in offshore wind farms (adapted from Thöns, 2018; Farhan et al., 2021). The tree consists of square nodes representing decisions, circular nodes representing random events or random variables, and diamond-shaped nodes representing utility.

and the maximum expected utility resulting the PA-DA, $\mathbb{E}[U_1|a^*]$, i.e.,

$$V_{\text{PA-DA}}^{\text{PIPA-DA}} = \mathbb{E}[U_2|i^*] - \mathbb{E}[U_1|a^*], \tag{4}$$

where $\mathbb{E}[U_2|i^*]$ and $\mathbb{E}[U_1|a^*]$ are determined as described in Appendix A.

The second DV, namely the predicted value of information and actions $V_{\text{SS-A}}^{\text{PIPA-DA}}$, is defined as the difference between the maximum expected utility resulting from the PIPA-DA, $\mathbb{E}[U_2|i^*]$, and the expected utility resulting from the SS-A, $\mathbb{E}[U_0]$:

$$V_{\text{SS-A}}^{\text{PIPA-DA}} = \mathbb{E}[U_2|i^*] - \mathbb{E}[U_0]. \tag{5}$$

The third DV, i.e., the predicted value of actions $V_{\text{SS-A}}^{\text{PA-DA}}$, is the difference between the maximum expected utility resulting from PA-DA and the expected utility provided by the SS-A given as

$$V_{\text{SS-A}}^{\text{PA-DA}} = \mathbb{E}[U_1|a^*] - \mathbb{E}[U_0]. \tag{6}$$

Essentially, an integrity management strategy should be implemented if the value of $V_{\text{PA-DA}}^{\text{PIPA-DA}}$, $V_{\text{SS-A}}^{\text{PIPA-DA}}$, or $V_{\text{SS-A}}^{\text{PA-DA}}$ is positive.

3   I&M of turbine support structures in offshore wind farms

3.1   I&M methods

Inspections are performed to obtain information on the condition of structural components. Concerning offshore wind turbine support structures, they look for (indicators of) deterioration (e.g., corrosion and/or fatigue cracks), which has an effect on the integrity of the structural systems. In this contribution, a probabilistic cost model is developed for I&M actions performed to detect and repair fatigue cracks in welded

connections in steel support structures of wind turbines in offshore wind farms (e.g., monopiles, jackets). In such structural systems, the welded components can be located above and below water level. The components located above water are typically part of the turbine tower, transition piece, main access platform, and access systems, which can be inspected via rope access and getting closer to the structure, while in the areas of the transition piece and substructure below water, inspections are carried out by a diver or by utilizing a remotely operated vehicle (ROV). The location of the inspected welded component thus has an effect on the required personnel, vessels, equipment, and logistics.

Two types of inspection methods to identify fatigue damage in welded components located above and/or below water level are considered: visual inspection and electromagnetic (EM) inspection methods such as eddy current (EC), magnetic particle inspection (MPI), and alternating current field measurement (ACFM). Visual inspection is a coarse method capable of detecting only relatively large surface breaking defects in welds or fatigue failures of welded connections. It can be performed with the help of a camera mounted on an ROV or by naked-eye observation. In contrast, EM inspection methods detect smaller surface breaking defects in welds. They can also be applied by a diver below water.

After an inspection campaign, if any fatigue damage is detected, a subsequent maintenance action (e.g., a repair) is performed based on the inspection outcomes. Depending on the criticality of the identified fatigue damage, the maintenance campaign is launched in the same year or the following year.

During an inspection campaign, the length and depth of a detected surface breaking defect are measured to inform decisions on the repair methods. With regards to possible repairs for welded joints, we consider two methods. The first repair method is referred to as welding (Rodriguez-Sanchez et al., 2011). In this method, the welded joint is repaired by removing a surface crack through grinding and subsequent filling of the resulting groove with wet welding. This method

is applied if the measured depth of the surface crack is greater than a defined percentage of the section thickness. Any surface crack with a measured depth less than the defined percentage of the section thickness may be repaired by grinding, which is the second repair method (Rodriguez-Sanchez et al., 2004).

3.2 Factors affecting I&M costs

There are several factors that influence the total cost of inspecting and maintaining support structures in an offshore wind farm. In this contribution, the influencing factors are identified, and their costs are estimated based on the existing scientific literature and interviews with I&M experts: a wind farm operator, engineering consultants, and operation and maintenance engineers – whose expertise does not necessarily cover all types of offshore wind farms. These experts are, however, able to provide sufficiently detailed information on established operational procedures and approximate estimates of I&M costs. The precise figures of I&M costs always depend on the actual wind farm type and the existing operational constraints. In this study, we consider the common case in which the wind farm is serviced by workboats operating from a nearby port base. Therefore, other forms of wind farm access such as helicopters are not considered in this contribution.

Accessibility is the main factor influencing the cost of I&M of turbine support structures in offshore wind farms. Depending on the location of the offshore wind farm, the type and location of the I&M activity (above water level (AW) and/or below water level (BW)), and the duration of the I&M activity, a certain type of vessel is employed. The choice of vessel for port-based operations could be a crew transfer vessel (CTV) or a service operation vessel (SOV). CTVs are usually used for frequent operations and are generally small aluminum catamarans employed to transfer personnel to and from offshore sites on a daily basis. CTVs do not have sufficient dynamic positioning redundancies to keep still during rough sea conditions. Their carrying capacity is usually 12 crew members who do 12 h shifts. SOVs are larger vessels designed and equipped to be present for a longer duration at the offshore wind farm for subsea or extensive I&M operations. These vessels have a capacity of around 40 technicians and can perform 24 h operations with multiple shifts (each shift is 12 h), which means that they come back to port only approximately once every 2 weeks (Martinez-Luengo and Shafiee, 2019). Table 1 shows the range of mobilization and demobilization costs as well as costs per shift for CTV and SOV.

The mobilization and demobilization costs of the vessels cover several aspects like the commuting time to the offshore wind farm, fuel consumption of the vessel, equipment and material costs, and project management costs, which account for logistics organization and reporting. The vessel cost per shift captures the number of people involved in the operation, the personnel costs, and the operational cost of the vessel during the I&M activity.

I&M also includes the additional effort for engineering the required repairs. This effort is associated with costs as summarized in Table 2. The engineering costs are usually dependent on the type of repair. In the case of grinding, the extra cost of engineering and preparation entails the design of the repair and laboratory tests among other factors. In the case of welding, the cost entails the design of the repair, chambers for underwater repair work if required, and laboratory tests. This additional cost is ideally incurred once during the service life of a wind farm because the type of hotspots and components is known; thus, if any repair is performed, the implementation of the repair has already been planned for the specific type of hotspot in the support structures.

The duration to complete an I&M activity is another factor that strongly influences the total I&M cost. It depends, for example, on the weather conditions, the experience of the personnel, the condition of the asset, and the existence of marine growth. The total time to complete an I&M activity usually entails transit time between WTs, the time required to complete the work package once stationed at a WT, and additional weather downtime due to unfavorable weather conditions. An increase in I&M activity time due to the aforementioned factors can lengthen the offshore time within a campaign. While this may not seem crucial, the time increase has an effect on other costs, such as the costs of the deployment of a vessel, personnel, and equipment. Table 3 shows the estimation of the time that each of the I&M activities takes for a single component in a support structure. A component is defined here as a hotspot in a welded connection (i.e., a certain section of a weld).

Weather downtime is mostly dependent on the type of vessel utilized and is given in Table 4. In the case of CTVs, the weather downtime is usually higher because they are small in size and lighter compared to SOVs and can easily lose position, especially if there are large waves and strong currents, while SOVs can safely withstand the harshest conditions even in winter.

The transit time between turbines also influences the inspection maintenance cost. It is estimated here based Martinez-Luengo and Shafiee (2019) and usually varies between 15 and 30 min.

Table 1. Estimates of vessel costs.

	Type of vessel	
Type of vessel cost	CTV	SOV
Mobilization/demobilization (EUR)	2000–20 000	15 000–80 000
Vessel cost per shift (EUR/shift)	1000–15 000	10 000–50 000

Table 2. Estimates of engineering costs.

Type of repair	Engineering cost (EUR)
Grind repair	5000–35 000
Weld repair	10 000–100 000

Table 3. I&M activity: type, location, and estimates of the duration per component.

Type of activity	Location	Hours per component
Weld repair	Above water	50–58
	Below water	60 – 70
Grind repair	Above water	14–18
	Below water	24–30
Visual inspection	Above water	1–2
	Below water	5–8
EM inspection	Above water	4–6
	Below water	10–15

Table 4. Estimates of weather downtime as a function of the vessel type.

Type of vessel	Weather downtime
CTV	30 %–40 %
SOV	10 %–15 %

4 Parametric model of I&M costs

4.1 Deterministic model

Based on the discussion of the factors affecting I&M costs in Sect. 3.2, we develop a deterministic parametric cost model to describe the total cost of I&M of WT support structures in an offshore wind farm. This cost can be generally broken down into a campaign cost C_C, engineering cost C_E, and operational cost C_{Op}. In the case that inspection and maintenance are performed simultaneously (mixed I&M), the total cost $C_{I\&M}$ is given as

$$C_{I\&M} = C_C + C_E + C_{Op}. \tag{7}$$

In the usual case where inspections and maintenance are performed in separate campaigns, the total cost of inspection C_I and the total cost of maintenance C_M are given by

$$C_I = C_C + C_{I,Op}$$
$$C_M = C_C + C_E + C_{M,Op}. \tag{8}$$

The campaign cost C_C corresponds to the fixed one-time cost of initiating the I&M activities, which includes the cost of commuting to the wind farm and back, the cost of the

equipment and materials required for the planned activities, fuel costs, and project management costs. These cost components are included in the mobilization and demobilization cost of the vessels (see Table 1). As discussed in Sect. 3.2, a CTV or SOV can be selected as a vessel for the planned I&M activities depending on their nature and extent. In the case of maintenance, an additional cost for planning and engineering repairs C_E has to be considered. This cost depends on the chosen repair method (welding or grinding).

Moreover, $C_{I,Op}$ and $C_{M,Op}$ are the operational costs of inspection and maintenance, which are the costs of conducting the inspection or maintenance operation when the vessel is at the offshore wind farm. The total operational costs further depend on the time to complete the operation, the vessel type, and its shift pattern. The total time to complete the operation depends on the extent of the I&M activity and where it is carried out, i.e., above or below water. The operational cost of inspection $C_{I,Op}$ and maintenance $C_{M,Op}$ activity is given by

$$C_{I,Op} = \frac{t_{I,Op}}{t_{shift}} \cdot C_{shift}$$
$$C_{M,Op} = \frac{t_{M,Op}}{t_{shift}} \cdot C_{shift}, \tag{9}$$

where C_{shift} is the cost of the vessel (CTV or SOV) per shift, t_{shift} is the duration of a shift (in hours) (see Sect. 3.2), $t_{I,Op}$ is the total time (in hours) to complete the overall inspection operation, and $t_{M,Op}$ is the total time to complete the overall maintenance operation. The total operational time for I&M is estimated as

$$t_{I,Op} = \left[\left[\sum_{i=1}^{n_{I,WT}} n_{I,C,i} \cdot t_{I,C} \right] + \left(n_{I,WT} - 1 \right) \cdot t_{transit} \right] \cdot (1 + WD)$$
$$t_{M,Op} = \left[\left[\sum_{i=1}^{n_{M,WT}} n_{M,C,i} \cdot t_{M,C} \right] + \left(n_{M,WT} - 1 \right) \cdot t_{transit} \right] \cdot (1 + WD), \tag{10}$$

where $n_{\mathrm{I,WT}}$ is the total number of WTs to be inspected in an offshore wind farm during an inspection campaign, $n_{\mathrm{M,WT}}$ is the total number of WTs to be repaired in the offshore wind farm during a maintenance campaign, $n_{\mathrm{I,C},i}$ is the number of components to be inspected in the ith WT support structure in the offshore wind farm, $n_{\mathrm{M,C},i}$ is the number of components to be repaired in the ith WT support structure in the offshore wind farm, t_{transit} is the transit time between the different WTs, $t_{\mathrm{I,C}}$ is the time to inspect a component above or below the water, and $t_{\mathrm{M,C}}$ is the time to repair a component above or below water. Furthermore, WD is the weather-related downtime, which is defined here relative to the overall operation time. This parameter also depends on the vessel type.

4.2 Probabilistic model

The model developed in Sect. 4 provides deterministic estimates of the I&M costs. However, due to the uniqueness of each operation and the complexity of the individual activities involved, the different parameters governing Eqs. (7), (8), (9), and (10) – i.e., the campaign cost, the vessel costs, the engineering costs, the inspection duration, the repair duration, the transit time, and the weather downtime – are uncertain and their values are typically only known in terms of intervals, as estimated in Sect. 3.2. To capture these uncertainties, the parameters of the cost model are modeled as random variables. By probabilistically modeling the uncertainties in the parameters and propagating them through the deterministic cost model, a probabilistic description of the I&M costs is obtained.

Let W generically denote the vector of random variables influencing the total I&M costs. Based on Eqs. (8), (9), and (10), the probabilistic cost model of inspection $C_{\mathrm{I}}(W)$ can now be written as

$$C_{\mathrm{I}}(W) = C_{\mathrm{C}} +$$
$$\frac{\left[\left[\sum_{i=1}^{n_{\mathrm{I,WT}}} n_{\mathrm{I,C},i} \cdot t_{\mathrm{I,C}}\right] + \left(n_{\mathrm{I,WT}} - 1\right) \cdot t_{\mathrm{transit}}\right] \cdot (1 + \mathrm{WD})}{t_{\mathrm{shift}}} \cdot C_{\mathrm{shift}}. \quad (11)$$

Similarly, the probabilistic cost model of maintenance $C_{\mathrm{M}}(W)$ is formulated as

$$C_{\mathrm{M}}(W) = C_{\mathrm{C}} + C_{\mathrm{E}}$$
$$+ \frac{\left[\left[\sum_{i=1}^{n_{\mathrm{M,WT}}} n_{\mathrm{M,C},i} \cdot t_{\mathrm{M,C}}\right] + \left(n_{\mathrm{M,WT}} - 1\right) \cdot t_{\mathrm{transit}}\right] \cdot (1 + \mathrm{WD})}{t_{\mathrm{shift}}}$$
$$\cdot C_{\mathrm{shift}}. \quad (12)$$

Given the lack of empirical data on the uncertain parameters of the cost models W, their probabilistic models are – in a Bayesian sense – chosen based on the available expert knowledge. It should be emphasized up front, however, that these probabilistic models can be updated using Bayesian methods if data on the parameters W become available.

As a first step in the probabilistic model building, the parameters in W are assumed to be independent and their
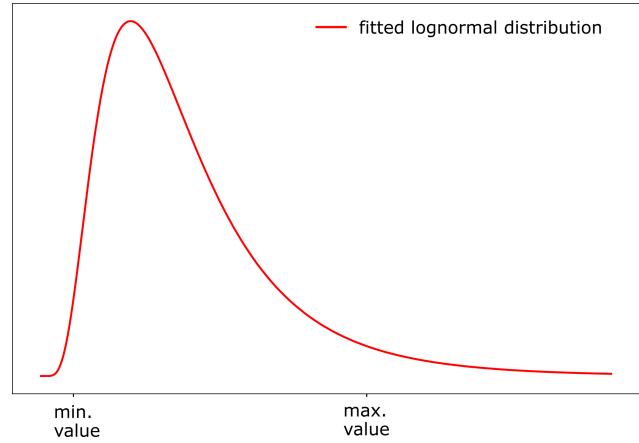

Figure 2. Lognormal distribution fitted based on the lower and upper bound on the corresponding cost model parameter. The lower and upper bounds represent the 1 % and 95 % quantile of the parameter values.

marginal distributions are assumed to follow a lognormal distribution. The first assumption is made as no information on the correlation of the different parameters is available. The second assumption is supported for the following reasons. First, each parameter of the cost models only takes non-negative values, and their statistical distribution is typically expected to be unimodal; i.e., one range of values in the distribution occurs more frequently than other ranges of values. A lognormal distribution is commonly chosen to probabilistically model such quantities as it is bounded by zero, has no upper limit, and is unimodal. Second, a lognormal distribution is skewed to the right with a long tail capturing rare extreme values of the cost model parameters. Third, the assumption that the parameters are lognormally distributed can be partially explained by the central limit theorem. Assuming that each parameter of the cost model itself derives from a multiplicative process, the sum of the logarithms of the factors in the underlying process approaches a normal distribution and their product approaches a lognormal distribution as the number of factors becomes large. For these reasons, a lognormal distribution is a plausible probabilistic model for the different cost model parameters (see also Moy et al., 2015).

As a second step in the model building, the statistics of the different lognormal distributions are determined based on the lower and upper bounds of each cost model parameter specified in Sect. 3.2. These bounds represent the available expert knowledge on the ranges of the parameter values. Based on additional expert judgement, the lower and upper bounds are assumed to characterize the 1 % and 95 % quantile of the parameter values. Using this information, the different lognormal distributions are fitted as illustrated in Fig. 2. The resulting mean and coefficient of variation (CoV) of each probabilistic parameter of the cost models are summarized Table 5.

Table 5. Mean and coefficient of variation (CoV) of the probabilistic parameters of the cost model.

Parameter	Description	Unit	Distribution	Mean	CoV
$C_{\mathrm{C,CTV}}$	Campaign cost (CTV)	[EUR]	lognormal	9111.04	0.63
$C_{\mathrm{C,SOV}}$	Campaign cost (SOV)	[EUR]	lognormal	43771.22	0.44
$C_{\mathrm{shift,CTV}}$	Vessel cost per shift (CTV)	[EUR/shift]	lognormal	6220.67	0.78
$C_{\mathrm{shift,SOV}}$	Vessel cost per shift (SOV)	[EUR/shift]	lognormal	27744.47	0.42
$t_{\mathrm{EM,BW}}$	Duration of component inspection (EM, below water)	[h]	lognormal	12.73	0.10
$t_{\mathrm{EM,AW}}$	Duration of component inspection (EM, above water)	[h]	lognormal	5.10	0.10
$t_{\mathrm{V,BW}}$	Duration of component inspection (visual inspection, below water)	[h]	lognormal	6.63	0.12
$t_{\mathrm{V,AW}}$	Duration of component inspection (visual inspection, above water)	[h]	lognormal	1.53	0.17
$C_{\mathrm{E,weld}}$	Engineering cost (welding)	[EUR]	lognormal	45719.43	0.63
$C_{\mathrm{E,grind}}$	Engineering cost (grinding)	[EUR]	lognormal	17584.96	0.51
$t_{\mathrm{weld,BW}}$	Duration of component repair (welding, below water)	[h]	lognormal	65.74	0.03
$t_{\mathrm{weld,AW}}$	Duration of component repair (welding, above water)	[h]	lognormal	54.59	0.03
$t_{\mathrm{grind,BW}}$	Duration of component repair (grinding, below water)	[h]	lognormal	27.41	0.05
$t_{\mathrm{grind,AW}}$	Duration of component repair (grinding above water)	[h]	lognormal	16.24	0.06
t_{transit}	Transit time between turbines	[h]	lognormal	0.38	0.17
$\mathrm{WD_{CTV}}$	Weather downtime (CTV)	–	lognormal	0.35	0.07
$\mathrm{WD_{SOV}}$	Weather downtime (SOV)	–	lognormal	0.12	0.10

5 Quantification of uncertainties in I&M costs and sensitivity analysis

5.1 Uncertainty quantification

The probabilistic cost models for I&M of turbine support structures in the offshore wind farm defined in Eqs. (11) and (12) can be applied for different combinations of input parameters. The different combinations are defined by the vessel type, the inspection and repair methods, the number of inspected and/or repaired components above and/or below water level, and the number of inspected and/or repaired wind turbine support structures. For illustration, the probabilistic total I&M costs are in the following quantified at wind farm, wind turbine, and component level.

First, the total I&M costs are estimated at wind farm level. To this end, it is assumed that $n_{\mathrm{I,C,BW}} = 1$ components of $n_{\mathrm{I,WT}} = 10$ support structures are inspected below water. In addition, it is assumed that $n_{\mathrm{M,C,BW}} = 5$ components of $n_{\mathrm{M,WT}} = 5$ support structures are repaired below water. Inspections are performed using EM and visual inspection methods, while welding and grinding are applied as repair methods. Moreover, a CTV is utilized as a workboat in each scenario. For each considered scenario, the probabilistic distributions of the total I&M costs are determined using Monte Carlo (MC) simulations with $n_{\mathrm{MC}} = 10^6$ samples of the corresponding model parameters. In the analysis, the model parameters are assumed to be statistically independent. The resulting empirical probability distributions of the total I&M costs are shown in Fig. 3.

Second, the total I&M costs are estimated at turbine level. In this case, it is assumed that 10 components of a support structure are inspected below water level, i.e., $n_{\mathrm{I,WT}} = 1$, $n_{\mathrm{I,C,BW}} = 10$, and 5 components in a support structure are re-

paired below water level, i.e., $n_{\mathrm{M,WT}} = 1$, $n_{\mathrm{M,C,BW}} = 5$. The assumptions regarding inspection and repair methods and the choice of vessel are the same as in the previous scenario considering I&M at wind farm level. The estimated empirical probability distributions of the total I&M costs together with their expected value and CoV are shown in Fig. 4.

Finally, the total I&M costs are estimated at the element level. In this scenario, $n_{\mathrm{I,C,BW}} = 1$ components of $n_{\mathrm{I,WT}} = 1$ turbines are inspected below water. The same is assumed for the maintenance campaign; i.e., only $n_{\mathrm{M,C,BW}} = 1$ component of $n_{\mathrm{M,WT}} = 1$ turbine support structure is repaired below water. The assumptions regarding inspection and repair methods and the choice of vessel are the same as in the scenario considering I&M at wind farm level. The empirical probability distributions of the total I&M costs are shown in Fig. 5.

From Figs. 3 to 5, it can be seen that propagating the uncertainties in the cost model parameters through the cost models defined in Eqs. (11) and (12) provides a probabilistic description of the total I&M costs. In each considered scenario, the total I&M costs exhibit an approximate lognormal distribution. The statistics of the total I&M costs shown in Figs. 3 to 5 are summarized in Table 6. Note that the coefficients of variation (CoVs) of the total I&M costs indicate that in each scenario certain parameters dominate the uncertainty in the total I&M costs. As an example, in Fig. 3a (wind-farm-level analysis considering EM inspection), the CoV of the total I&M costs is similar to the CoV of the vessel cost per shift. This finding is further substantiated by the variance-based sensitivity analysis in Sect. 5.2.1, where in Fig. 6 we observe that the vessel cost per shift has a sensitivity index close to 1 for the same inspection scenario.
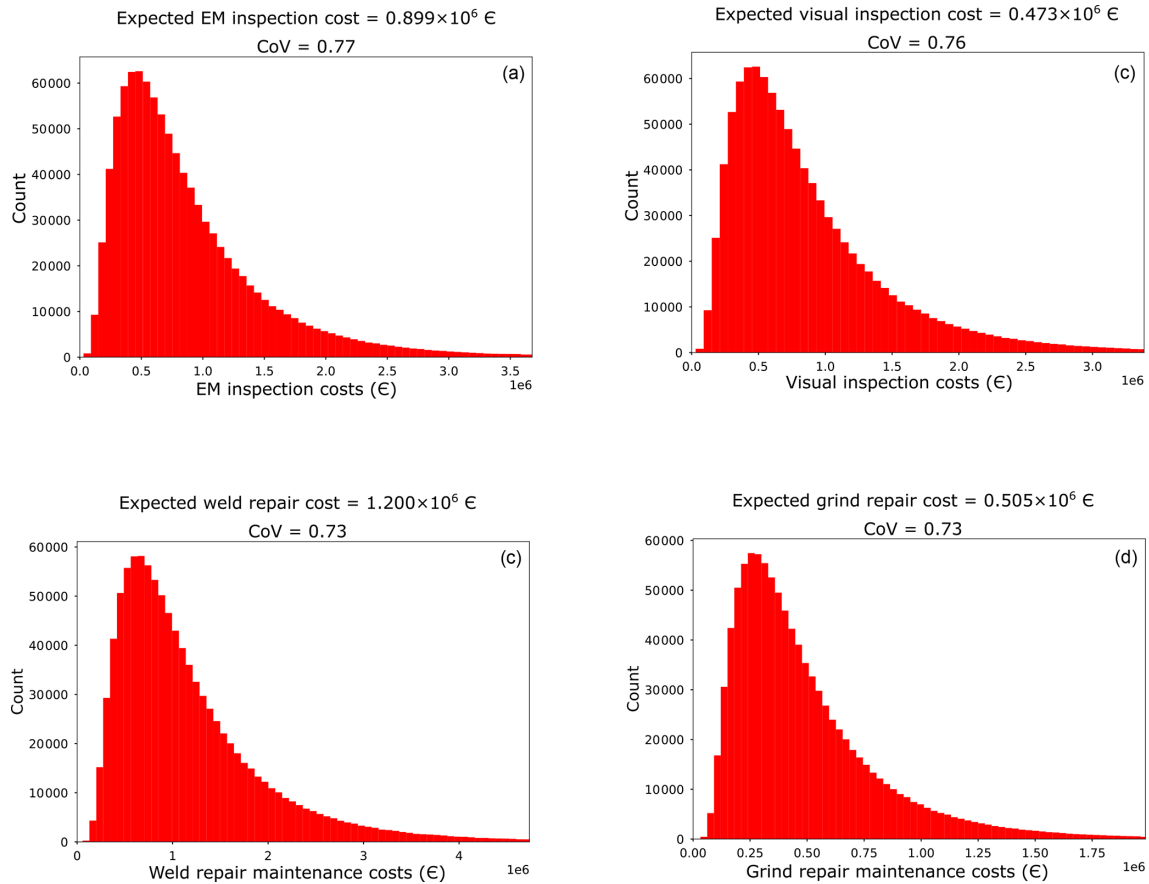
Figure 3. Empirical probability distributions of the total I&M costs: **(a)** 10 components in each group of 10 support structures are inspected below water with EM inspection technique, **(b)** 10 components in each group of 10 support structures are visually inspected below water, **(c)** 5 components in each group of 5 support structures are repaired below water by welding, and **(d)** 5 components in each group of 5 support structures are repaired below water by grinding.

Table 6. Summary of the statistics of the total I&M costs.

		Wind farm	Wind turbine	Component
EM inspection	Expected value (EUR 10^6)	0.899	0.097	0.018
	CoV	0.77	0.70	0.50
Visual inspection	Expected value (EUR 10^6)	0.473	0.055	0.014
	CoV	0.76	0.66	0.49
Weld repair	Expected value (EUR 10^6)	1.200	0.283	0.100
	CoV	0.73	0.63	0.45
Grind repair	Expected value (EUR 10^6)	0.505	0.122	0.046
	CoV	0.73	0.60	0.39

5.2 Sensitivity analysis

As discussed in Sects. 3 and 4, the total I&M costs are influenced by numerous uncertain parameters W. To study the importance of each model parameter W_i, a variance-based sensitivity analysis is performed (Sobol, 1993), which quantifies the effect of W_i on the variance of the inspection and maintenance costs in terms of the following first-order measure:

$$V_i = \mathrm{Var}_{W_i}\left\{\mathbb{E}_{W_{-i}}[C(W)|W_i]\right\}, \tag{13}$$

where $C(W)$ can be the probabilistic model of the inspection costs defined in Eq. (11) or the probabilistic model of
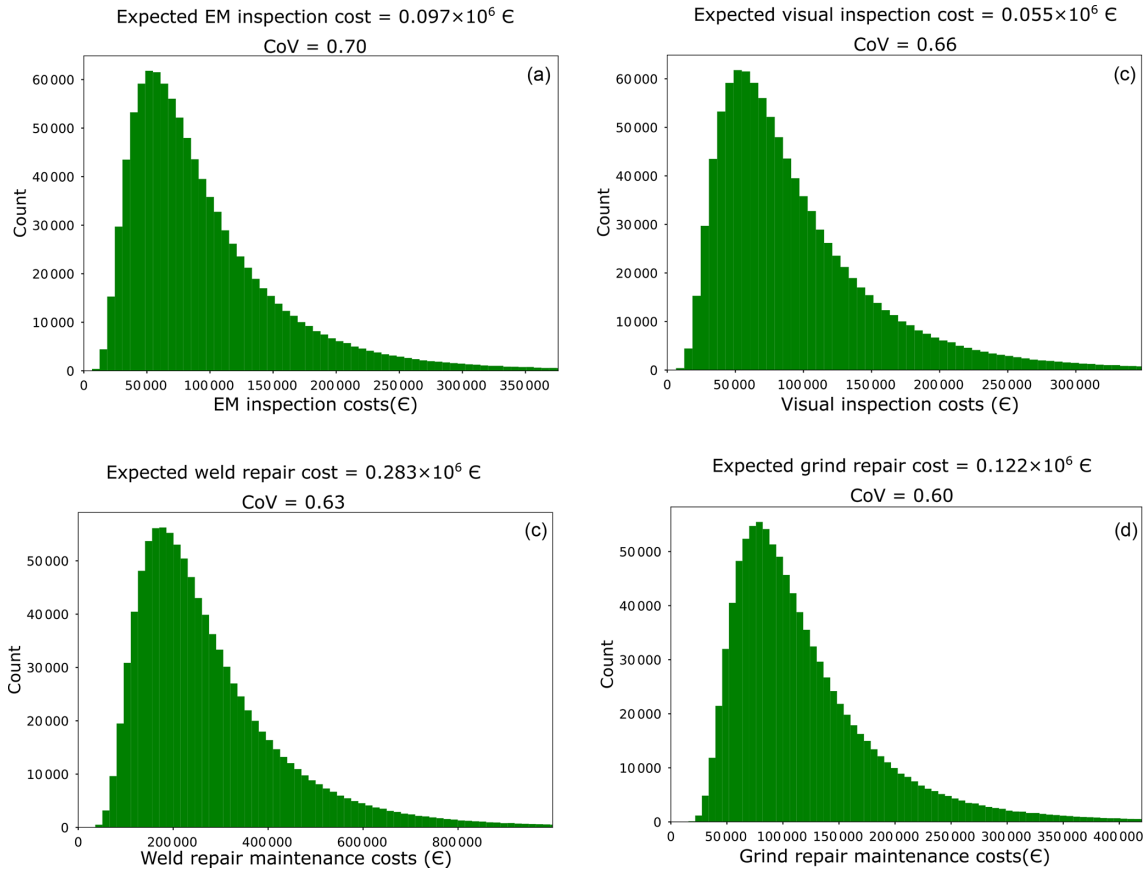
Figure 4. Empirical distributions of the total I&M costs: **(a)** 10 components of a turbine support structure are inspected below water with the EM inspection technique, **(b)** 10 components of a turbine support structure are visually inspected below water, **(c)** 5 components of a turbine support structure are repaired below water by welding, and **(d)** 5 components of a turbine support structure are repaired below water by welding.

the maintenance costs defined in Eq. (12), $\mathbb{E}_{W_{-i}}[C(W)|W_i]$ is the expected value of the inspection or maintenance costs with respect to all parameters except W_i whose value is fixed, and $\mathrm{Var}_{W_i}\{\mathbb{E}_{W_{-i}}[C(W)|W_i]\}$ is the variance of this average model. Normalizing V_i with the variance $\mathrm{Var}[C(W)]$ provides the first-order sensitivity index S_i (Sobol, 1993):

$$S_i = \frac{V_i}{\mathrm{Var}[C(W)]} = \frac{\mathrm{Var}_{W_i}\{\mathbb{E}_{W_{-i}}[C(W)|W_i]\}}{\mathrm{Var}[C(W)]}, \qquad (14)$$

in which $\mathrm{Var}[C(W)]$ is the variance of the inspection or maintenance costs. S_i is evaluated here using an MC approach (Sobol, 2001).

5.2.1 Inspection costs

The first part of the sensitivity study analyzes the effect of the campaign cost C_c, vessel cost per shift C_{shift}, and inspection operation time $t_{\mathrm{I,Op}}$ on the total inspection costs based on the probabilistic cost model defined in Eq. (11), where the inspection operation time depends on the duration of a com-

ponent inspection, the transit time between turbines, and the weather downtime.

For the inspection campaign, we perform a sensitivity analysis assuming that inspections are performed using the EM inspection method via a CTV. The study explores various scenarios related to component location (above or below water), the number of inspected turbine support structures, and the quantity of inspected components within each structure. Figure 6 illustrates these scenarios, with columns representing the number of inspected turbines and rows corresponding to component location. Each panel displays sensitivity indices for campaign cost, vessel operation cost, and inspection operation time as functions of the number of inspected components.

Figure 6 reveals that the vessel cost per shift exerts the most significant impact on total inspection cost throughout various scenarios, while the inspection operation time has the smallest effect. Campaign costs only become significant when a few components are inspected in one WT support structure. We obtain similar results when considering visual
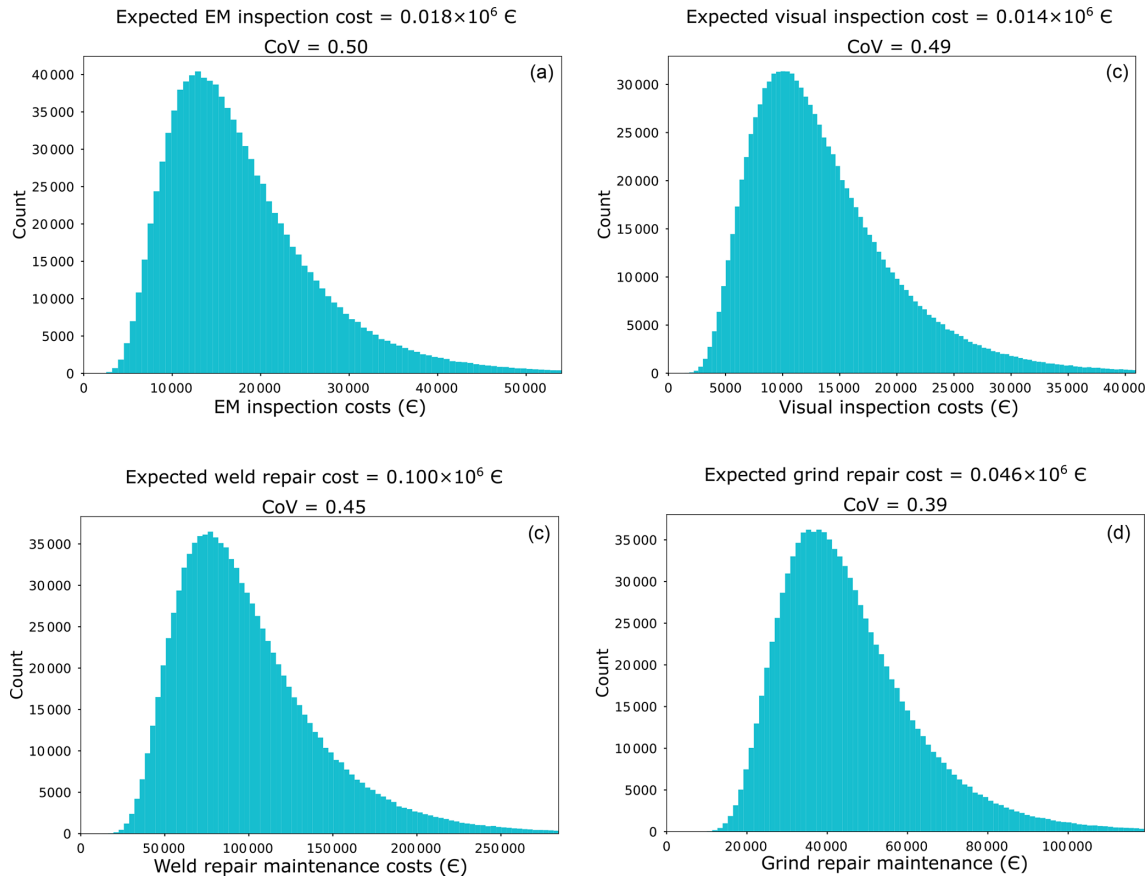
Figure 5. Empirical distributions of the total I&M costs: **(a)** EM inspection of a component in a support structure below water level, **(b)** visual inspection of a component in a support structure below water level, **(c)** welding repair maintenance of a component repaired below water level for a support structure, and **(d)** grinding repair maintenance of a component repaired below water level for a support structure.

inspections as the inspection method and an SOV as a workboat.

5.2.2 Maintenance costs

The second part of our sensitivity study evaluates the impact of the campaign cost C_c, the engineering costs C_E, the vessel cost per shift C_{shift}, and repair operation time $t_{M,Op}$ on the maintenance costs defined by Eq. (12). In the analysis, we assume that welding is used as the repair method and a CTV is utilized as the workboat. The study considers various scenarios related to the component location (above or below water), the number of repaired turbine support structures, and the number of repaired components within each support structure.

In Fig. 7, we observe that at the turbine level the engineering costs have the greatest impact on the total maintenance costs, while the other parameters only have a small influence. Additionally, the influence of the vessel cost per shift increases with the number of repaired turbines and components, while the impact of the engineering costs decreases.

Similar results are obtained when considering grinding as the repair method and an SOV as a workboat.

6 Numerical example

In the following, the probabilistic cost model formulated in Sect. 4 is applied in a cost- and risk-informed optimization of an I&M strategy for the two-dimensional steel frame resembling a jacket support structure of an offshore wind turbine (see Fig. 8). The optimization is performed at the beginning of its lifetime based on information from the design phase. The frame has been studied in numerous publications, and in the following we provide a summary of the underlying models and assumptions. A more detailed description of the frame can be found in Schneider et al. (2017), Schneider (2020), and Eichner et al. (2023).

The steel frame is made of welded tubular sections. Its planned lifetime is 25 years, which is divided into $j = 1, \ldots, m$ intervals of 1 year length. During the operational phase, the frame is exposed to a time-dependent lateral force representing a storm load. This load is modeled by its annual maximum $L_{max,j}$. In addition to storm loads, the frame
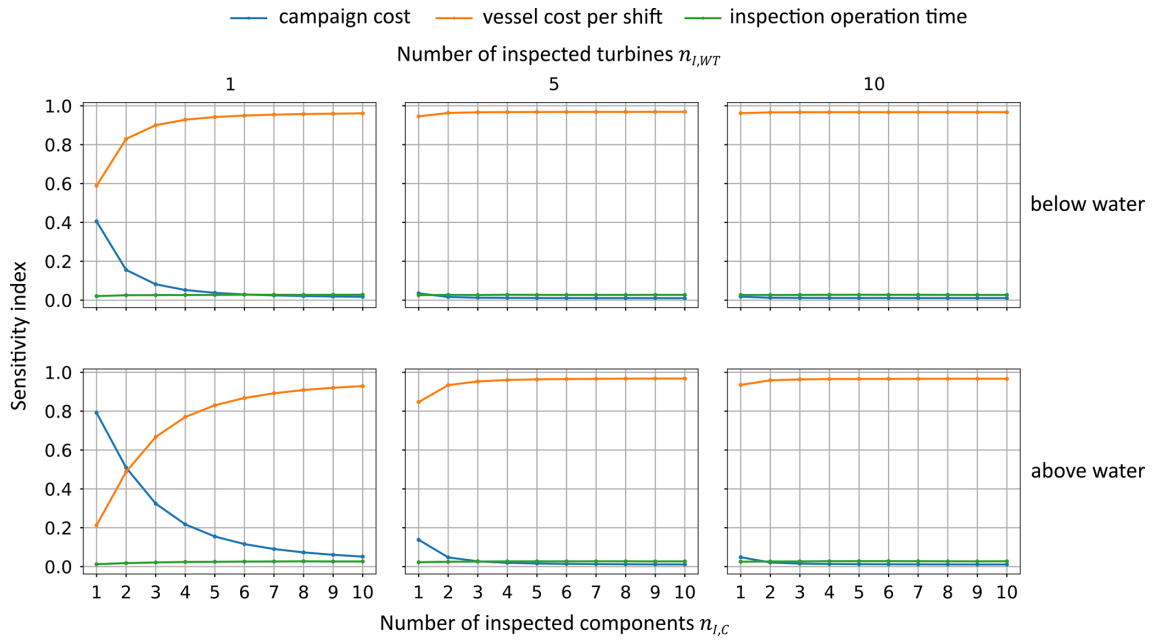
Figure 6. Sensitivity indices of the campaign cost C_c, vessel cost per shift C_{shift}, and inspection operation time $t_{I,Op}$ as a function of the location of the inspected components (above or below water), the number of inspected turbine support structures, and the number of inspected components in each support structure. Inspections are performed using the EM inspection method via a CTV.
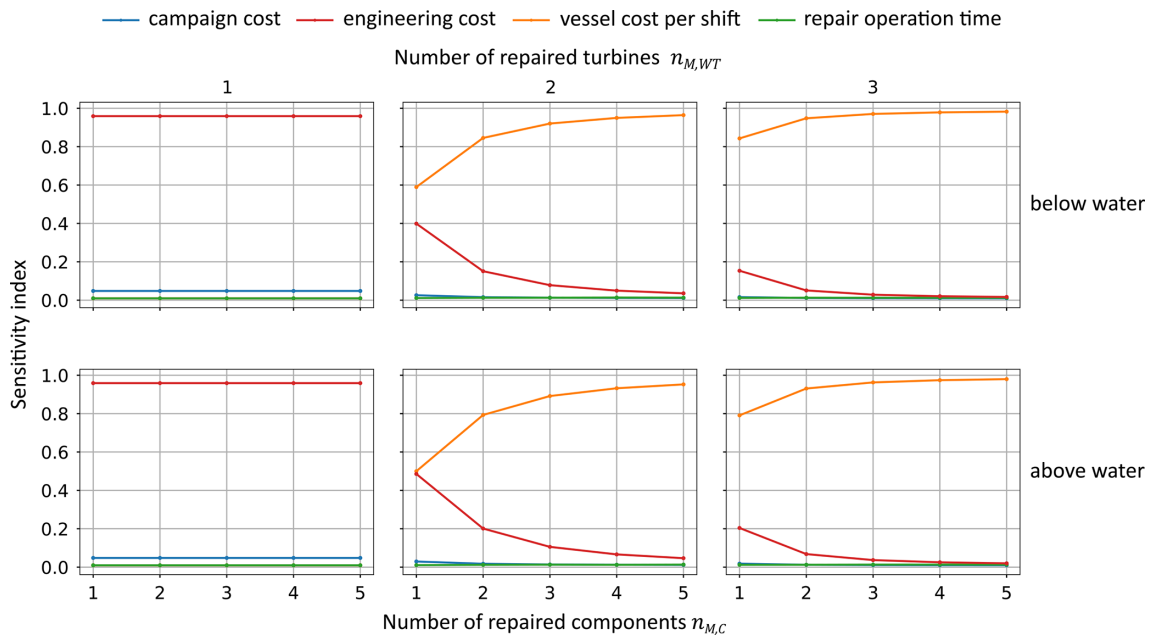

Figure 7. Sensitivity indices of the campaign cost C_c, the cost of engineering repairs C_E, the vessel cost per shift C_{shift}, and the repair operation time $t_{M,Op}$ as a function of the location of the repaired components (above or below water), the number of repaired turbine support structures, and the number of repaired components in each support structure. Repairs are performed using the welding repair method and a CTV.

– like a jacket support structure of an offshore wind turbine – is subject to fatigue due to dynamic excitations. In the current analysis, the welded connections of the frame contain 22 critical fatigue hotspots, which are indicated as red dots in Fig. 8. The hotspot fatigue demand is quantified by the corresponding distributions of the fatigue stress ranges. Typically, these distributions are derived from an overall dynamic response analysis. In the current example, they are – as described in Straub (2004) – determined based on the available design information (i.e., the hotspot fatigue lives and the applied SN curves).

Fatigue deterioration of the hotspots is described by probabilistic Paris–Erdogan fatigue crack growth models. The statistical dependence among the fatigue behavior of different hotspots is captured by introducing correlations among the uncertain parameters of the hotspot fatigue models. This correlation influences the system reliability and has an impact on the (optimal) inspection and maintenance regime.

The hotspots are inspected with MPI via a CTV and repaired by welding if required. The applied repair model is documented in detail in Farhan et al. (2021). It is assumed that hotspots 1 to 8 are located above water, while hotspots 9 to 22 are located below water. The location of the hotspots (above or below water) influences the cost of inspections and repairs.

The time-dependent failure probability is computed by coupling the probabilistic fatigue deterioration models with a probabilistic structural performance model utilized to evaluate the system failure probability conditional on the hotspot condition. Inspection information is included in the estimation of the system failure probability through Bayesian updating of the probabilistic fatigue models. Further information regarding the applied fatigue, structural performance, and inspection models as well as the methods employed to compute the (updated) time-variant failure probability of the frame is documented (Schneider et al., 2017; Schneider, 2020; Eichner et al., 2023).

In the current application, all consequences (costs of inspections and repairs as well as failure consequences) are expressed as monetary costs C to facilitate quantitative DV analyses. Furthermore, as discussed in Nielsen and Sorensen (2021), the economic benefits from the existence of the wind turbine may be assumed to be independent of the structural reliability and I&M actions. In this case, they are constant and, consequently, can be neglected in the optimization of I&M of the WT support structure. It follows that the utility U introduced in Sect. 2.1 is proportional to $-C$.

6.1 System state analysis

The SS-A determines the expected total lifetime cost $\mathbb{E}[C_0]$ assuming that no inspections and no maintenance actions are performed during the lifetime of the support structure. $\mathbb{E}[C_0]$ is equal to the expected total lifetime cost of system failure
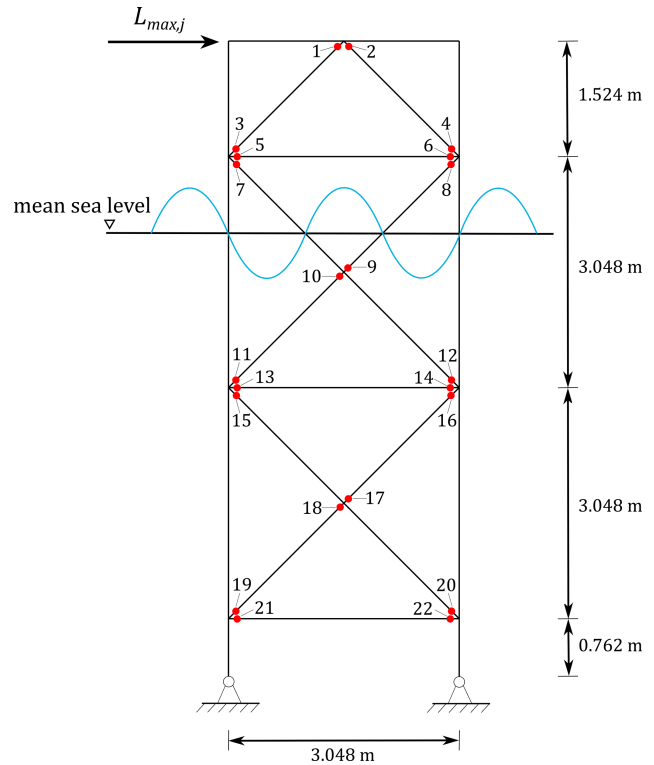

Figure 8. Steel frame with 22 fatigue hotspots indicated as red dots (adapted from Schneider et al., 2017).

$\mathbb{E}[C_F]$ (lifetime risk of failure), i.e.,

$$\mathbb{E}[C_0] = \mathbb{E}[C_F] = \sum_{j=1}^{m} c_F \cdot \gamma_j \cdot \left[\Pr(F_j) - \Pr(F_{j-1}) \right], \quad (15)$$

where $c_F = \text{EUR} \, 2 \times 10^7$ is the failure cost, which is assumed here to be deterministic and equal to the investment cost of one wind turbine (Thöns et al., 2017); $\Pr(F_j)$ is the cumulative probability of failure up to the end of year j; $\Pr(F_j) - \Pr(F_{j-1})$ is the probability of failure in year j; and γ_j is the discounting function, which discounts the failure cost c_F occurring in year j back to the present. The discounting function is defined as $\gamma_j = 1/(1+r)^j$, wherein $r = 0.02$ is the discount rate. The expected total lifetime cost $\mathbb{E}[C_0]$ of the case study related to the steel frame is EUR 7×10^5.

6.2 Predictive information and predictive action decision analysis considering probabilistic I&M costs

The PIPA-DA for jointly optimizing I&M is performed using the heuristic cost- and risk-informed approach proposed in Luque and Straub (2019) and Bismut and Straub (2021), which corresponds in essence to the normal form of the preposterior decision analysis. We adopt this approach as it is computationally tractable compared to the extensive form of analysis described in Appendix A3. In this approach, an

I&M strategy, generically denoted by $\mathcal{S}$, is defined by parameterized rules that specify what, when, and how to inspect and repair based on the available system information (i.e., inspection outcomes and corresponding repairs as well as the predicted system failure probability conditional on the inspection outcomes and previously performed repairs). In the current application, the parameterized rules are defined as follows (see also Bismut et al., 2017; Eichner et al., 2023; Schneider, 2019).

1. Inspection campaigns are performed at fixed intervals Δt.

2. $n_{I,C}$ hotspots are inspected during each inspection campaign.

3. Hotspots are prioritized for inspection according to a metric proposed by Bismut et al. (2017), which is a function of a parameter η as well as the structural importance and fatigue reliability of each hotspot.

4. An additional inspection campaign is launched if the predicted annual system failure probability exceeds a threshold p_{th}.

5. A maintenance campaign is launched if fatigue cracks are indicated and measured to be deeper than a_R.

Note that rules 4 and 5 have the following implication: inspection information obtained at one hotspot contains indirect information on the fatigue state of the remaining hotspots as their fatigue behavior is correlated due to common influencing factors (see Straub and Faber, 2004, for a detailed discussion). Now consider the case in which a fatigue crack is unexpectedly indicated at one hotspot and measured to be deeper than a_R. Conditional on this inspection information, the probability that fatigue deterioration of the remaining hotspots has progressed faster than expected increases. Consequently, the system failure probability also increases. If it exceeds the threshold p_{th}, additional inspections and possibly repairs are performed as prescribed by rules 4 and 5. Because of these two rules and the explicit modeling of the dependence among the fatigue behavior of different hotspots, the current optimization of I&M of the frame captures scenarios in which the inspection and repair effort has to be increased due to accelerated fatigue deterioration.

From the above list of parameterized rules, it follows that the I&M strategy $\mathcal{S}$ is fully defined here by the parameters $\boldsymbol{\theta} = \left[\Delta t, p_{th}, n_{I,C}, \eta, a_R \right]^T$. To highlight the dependence of $\mathcal{S}$ on $\boldsymbol{\theta}$, we write $\mathcal{S}_{\boldsymbol{\theta}}$ in the following.

The utility function – or more precisely the cost function – underlying the current optimization is (generically) defined as

$$C_2(\mathcal{S}_{\boldsymbol{\theta}}, \boldsymbol{X}, \boldsymbol{Y}, \boldsymbol{Z}, \boldsymbol{W}) = C_I(\mathcal{S}_{\boldsymbol{\theta}}, \boldsymbol{X}, \boldsymbol{Y}, \boldsymbol{Z}, \boldsymbol{W})$$
$$+ C_M(\mathcal{S}_{\boldsymbol{\theta}}, \boldsymbol{X}, \boldsymbol{Y}, \boldsymbol{Z}, \boldsymbol{W}) + C_F(\mathcal{S}_{\boldsymbol{\theta}}, \boldsymbol{X}, \boldsymbol{Y}, \boldsymbol{Z}, \boldsymbol{W}), \quad (16)$$

where $C_2(\mathcal{S}_{\boldsymbol{\theta}}, \boldsymbol{X}, \boldsymbol{Y}, \boldsymbol{Z}, \boldsymbol{W})$ is the total lifetime cost, $C_I(\mathcal{S}_{\boldsymbol{\theta}}, \boldsymbol{X}, \boldsymbol{Y}, \boldsymbol{Z}, \boldsymbol{W})$ is the total lifetime inspection cost, $C_M(\mathcal{S}_{\boldsymbol{\theta}}, \boldsymbol{X}, \boldsymbol{Y}, \boldsymbol{Z}, \boldsymbol{W})$ is the total lifetime maintenance cost, and $C_F(\mathcal{S}_{\boldsymbol{\theta}}, \boldsymbol{X}, \boldsymbol{Y}, \boldsymbol{Z}, \boldsymbol{W})$ is the total lifetime cost of structural failure. These costs are defined as a function of the I&M strategy $\mathcal{S}_{\boldsymbol{\theta}}$, the uncertain parameters $\boldsymbol{X}$ influencing the time-dependent system failure probability, the uncertain parameters $\boldsymbol{Y}$ influencing the effect of repairs, and the uncertain parameters of the I&M cost model $\boldsymbol{W} = \left[\boldsymbol{W}_1^T, ..., \boldsymbol{W}_m^T \right]^T$, where $\boldsymbol{W}_j$ represents the uncertain parameters influencing the I&M costs in year j as defined in Table 5. The total I&M costs occurring in each year j are evaluated based on the parametric cost models described in Sect. 4. It is assumed here that the different $\boldsymbol{W}_j$, $j = 1, ..., m$ values are independent and identically distributed. Note that this assumption is not a limitation, as the model can be extended to account for dependent and non-identically distributed cost model parameters.

The optimal strategy $\mathcal{S}_{\boldsymbol{\theta}*}$ characterized by the optimal heuristic parameters $\boldsymbol{\theta}^*$ minimizes the expected value of the total lifetime cost $\mathbb{E}[C_2|\mathcal{S}_{\boldsymbol{\theta}}] = \mathbb{E}_{X,Y,Z,W}[c_2(\mathcal{S}_{\boldsymbol{\theta}}, \boldsymbol{X}, \boldsymbol{Y}, \boldsymbol{Z}, \boldsymbol{W})]$. It follows that the optimal heuristic parameters $\boldsymbol{\theta}^*$ can be determined as

$$\boldsymbol{\theta}^* = \arg\min_{\boldsymbol{\theta}} \mathbb{E}[C_2|\mathcal{S}_{\boldsymbol{\theta}}]. \quad (17)$$

$\mathbb{E}[C_2|\mathcal{S}_{\boldsymbol{\theta}}]$ is evaluated as described in Appendix B1. The optimal heuristic parameters $\boldsymbol{\theta}^*$ are identified here by conducting an exhaustive search across the following sets of parameter values: $\Delta t \in \{4, 8\}$ [years], $p_{th} \in \{5 \times 10^{-4}, 10^{-3}\}$, $n_{I,C} \in \{1, ..., 22\}$, $\eta = 1$, and $a_R = 1$ [mm]. The estimated expected total lifetime cost $\mathbb{E}[C_2|\mathcal{S}_{\boldsymbol{\theta}}]$ as a function of $\boldsymbol{\theta}$ is shown in Fig. 9.

All strategies with $n_{I,C} = \{3, 4, 5, 6\}$ result in a similar expected total lifetime cost. This provides some flexibility to the decision-maker to choose a strategy based on their specific requirements regarding the inspection interval and structural reliability. Notably, both strategies with $\Delta t = 4$ years exhibit similar expected costs for $n_{I,C} > 7$ regardless of the reliability threshold. When considering strategies with $\Delta t = 8$, the reliability threshold has an impact on the expected total lifetime cost: a lower threshold results in more unscheduled inspections between regular inspections. In our current example the optimal strategy $\mathcal{S}_{\boldsymbol{\theta}*}$ is characterized by $\boldsymbol{\theta}^* = \left[\Delta t = 8, p_{th} = 1 \times 10^{-3}, n_{I,C} = 6, \eta = 1, a_R = 1 \right]^T$.

Figure 10 shows the decomposed expected total lifetime cost $\mathbb{E}[C_2|\mathcal{S}_{\boldsymbol{\theta}}]$ as a function of the heuristic parameters $\boldsymbol{\theta} = \left[\Delta t = 8, p_{th} = 1 \times 10^{-3}, n_{I,C} = 1, ..., 22, \eta = 1, a_R = 1 \right]^T$. This cost is composed of the expected values of the failure cost, inspection campaign cost, inspection operation cost, repair campaign cost, repair operation cost, and engineering cost for repairs. As the inspection effort increases (i.e., more hotspots are inspected during each inspection campaign), the expected value of the system failure cost
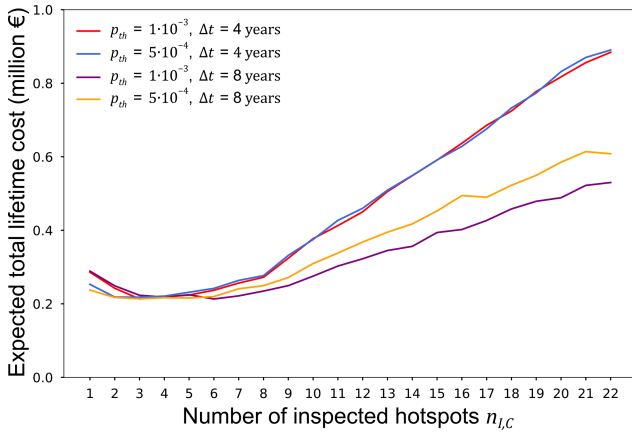
Figure 9. Expected total lifetime cost $\mathbb{E}\left[C_2|S_\theta\right]$ as a function of $\theta = \left[\Delta t, p_{\text{th}}, n_{\text{I,C}}, \eta, a_R\right]^T$ determined based on the probabilistic I&M cost model.
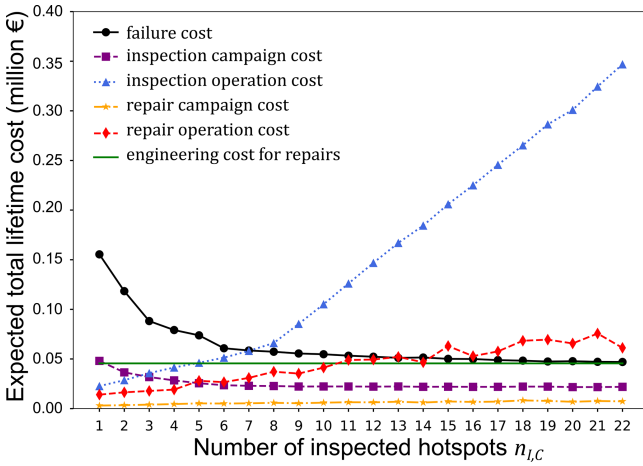

Figure 10. Decomposed expected total lifetime cost $\mathbb{E}\left[C_2|S_\theta\right]$ as a function of $\theta = \left[\Delta t = 8, p_{\text{th}} = 1 \times 10^{-3}, n_{\text{I,C}} = 1, \ldots, 22, \eta = 1, a_R = 1\right]^T$.

(i.e., the risk of structural failure) decreases, and – as expected – the expected values of the inspection and repair costs increase. This nicely illustrates the impact of the risk mitigation measures on the structural risk of failure. Note that the engineering cost for repairs is constant in this case study since it is incurred here only once at the beginning of the operational phase as repair solutions are engineered proactively before the frame is commissioned. Consequently, they could be neglected in the current optimization, as they only shift the expected total lifetime costs upwards by a fixed value.

To support the decision on whether one should implement an I&M strategy, the predicted value of information and actions is computed by the difference between the expected total lifetime cost $\mathbb{E}[C_0]$ and the expected total lifetime cost $\mathbb{E}[C_2|S_\theta]$. By normalizing this difference with respect to $\mathbb{E}[C_0]$, the relative $\overline{V}_{\text{SS-A}}^{\text{PIPA-DA}}(\theta)$ is obtained (Farhan et al.,
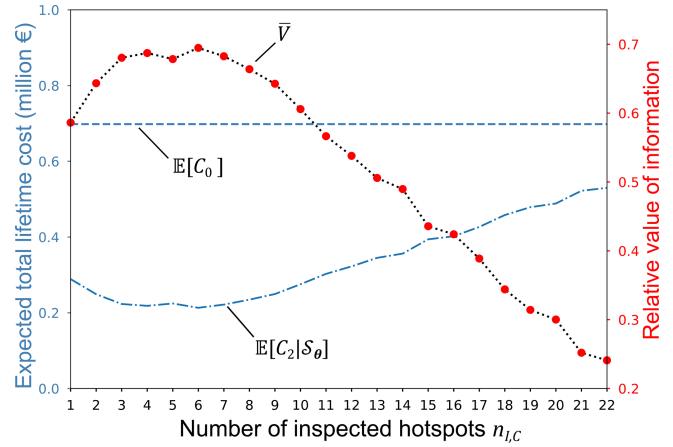

Figure 11. Relative DV $\overline{V}_{\text{SS-A}}^{\text{PIPA-DA}}(\theta) = (\mathbb{E}[C_0] - \mathbb{E}[C_2|S_\theta])/\mathbb{E}[C_0]$ together with the expected lifetime costs $\mathbb{E}[C_2|S_\theta]$ as a function of $\theta = \left[\Delta t = 8, p_{\text{th}} = 1 \times 10^{-3}, n_{\text{I,C}} = 1, \ldots, 22, \eta = 1, a_R = 1\right]^T$ and $\mathbb{E}[C_0]$.

2021):

$$\overline{V}_{\text{SS-A}}^{\text{PIPA-DA}}(\theta) = \frac{\mathbb{E}[C_0] - \mathbb{E}[C_2|S_\theta]}{\mathbb{E}[C_0]}. \tag{18}$$

Figure 11 shows the $\overline{V}_{\text{SS-A}}^{\text{PIPA-DA}}$ as a function of the parameters $\theta = \left[\Delta t = 8, p_{\text{th}} = 1 \times 10^{-3}, n_{\text{I,C}} = 1, \ldots, 22, \eta = 1, a_R = 1\right]^T$, where $\Delta t = 8$ and $p_{\text{th}} = 1 \times 10^{-3}$ are the optimal inspection interval and reliability threshold. The dashed blue line corresponds to the expected total lifetime cost $\mathbb{E}[C_0]$ determined by the SS-A. The dashed–dotted blue line corresponds to the expected total lifetime cost $\mathbb{E}[C_2|S_\theta]$. Notably, $\overline{V}_{\text{SS-A}}^{\text{PIPA-DA}}$ is positive for $n_{\text{I,C}} = 1, \ldots, 22$. This result indicates that it is a rational decision to inspect and maintain the frame. As expected, the highest $\overline{V}_{\text{SS-A}}^{\text{PIPA-DA}}$ is obtained when implementing the optimal strategy $S_{\theta*}$ with an optimal number of inspected hotspots in each inspection campaign $n_{\text{I,C}} = 6$.

6.3 Predictive information and predictive action decision analysis considering expected I&M costs

The numerical example considers only a single turbine support structure. In this case, the cost models defined in Eqs. (11) and (12) can be expressed as linear functions of the number of inspected and repaired hotspots as follows:

$$C_{\text{I}} = C_{\text{C}} + n_{\text{I,C}} \cdot C_{\text{I,Op}} \text{ with}$$

$$C_{\text{I,Op}} = \frac{t_{\text{I,C}} \cdot (1 + \text{WD}) \cdot C_{\text{shift}}}{t_{\text{shift}}} \tag{19}$$

and

$$C_{\text{M}} = C_{\text{C}} + C_{\text{E}} + n_{\text{M,C}} \cdot C_{\text{M,Op}} \text{ with}$$

$$C_{\text{M,Op}} = \frac{t_{\text{M,C}} \cdot (1 + \text{WD}) \cdot C_{\text{shift}}}{t_{\text{shift}}}. \tag{20}$$
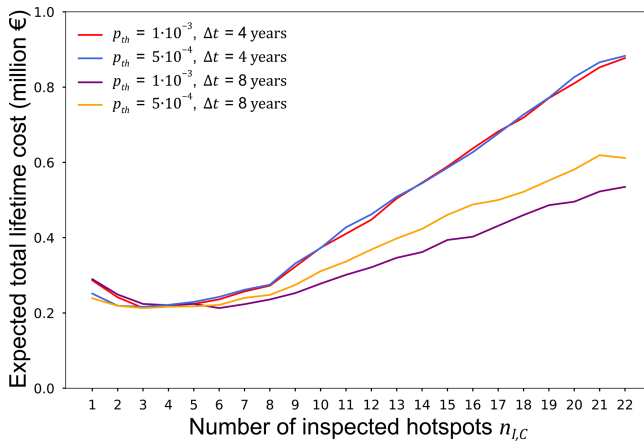
Figure 12. Expected total lifetime cost $\mathbb{E}[C_2|\mathcal{S}_\theta]$ as a function of $\theta = \begin{bmatrix} \Delta t, p_{\text{th}}, n_I, \eta, a_R \end{bmatrix}^T$ determined based on the expected values of the parameters of the I&M cost model.

The expected lifetime cost $\mathbb{E}[C_2|\mathcal{S}_\theta]$ can now be estimated based on the expected values of the parameters of the I&M cost model as described in Appendix B2. Subsequently, the optimal heuristic parameters θ^* are identified based on Eq. (17) by again conducting an exhaustive search across the following sets of parameter values: $\Delta t \in \{4, 8\}$ [years], $p_{\text{th}} \in \{5 \times 10^{-4}, 10^{-3}\}$, $n_{I,C} \in \{1, \ldots, 22\}$, $\eta = 1$ and $a_R = 1$ [mm]. The estimated expected total lifetime cost $\mathbb{E}[C_2|\mathcal{S}_\theta]$ considering expected I&M costs is shown in Fig. 12.

It can be seen that the current analysis provides the same results as the analysis considering the probabilistic I&M costs (see also Fig. 9) and thus the same optimal strategy $\mathcal{S}_{\theta^*}$ with $\theta^* = \begin{bmatrix} \Delta t = 8, p_{\text{th}} = 1 \times 10^{-3}, n_{I,C} = 6, \eta = 1, a_R = 1 \end{bmatrix}^T$. Consequently, the current analysis illustrates that the I&M costs can be considered deterministically as expected values in the DV analysis if they are included in the optimization on a linear basis.

Aligning with existing works, we utilize the probabilistic I&M cost model to derive deterministic or normalized cost ratios. In the literature, such a normalization is typically performed with respect to the failure cost or expected campaign cost due to their significant contribution to the overall lifetime costs. Applying the same methodology, we obtain the normalized cost models summarized in Tables 7 and 8. These models can subsequently be used to optimize I&M of offshore wind turbine support structures if the costs are included in the underlying models on a linear basis.

7 Summary and concluding remarks

This paper formulates and applies a probabilistic cost model to support the planning of I&M of the turbine support structures in offshore wind farms. It provides a decision-theoretical basis for optimizing I&M activities, with an emphasis on integrating the probabilistic cost model in the deci-

sion analysis. The probabilistic cost model is derived based on a discussion of (a) the types of I&M of turbine support structures and (b) the parameters that influence the overall I&M cost. Subsequently, variance-based sensitivity analyses are performed based on the probabilistic cost model to quantify the influence of the different cost model parameters on the overall I&M costs. Finally, the proposed probabilistic cost model is applied in a numerical example in which the I&M regime is optimized for a frame with steel members which resembles a jacket support structure of an offshore wind turbine. As part of the example, an SS-A, PIPA-DA, and DV analysis is performed. The SS-A determines the lifetime risk of structural failure when no information is collected, and no maintenance actions are performed throughout the structure's lifetime. The PIPA-DA optimizes a heuristic I&M strategy defined by parameterized rules that guide the actions to be taken based on the available system information. The analysis is first performed based on the probabilistic model of the I&M costs. Subsequently, it is performed based on the expected values of the I&M costs. This is possible here since the costs are included in the model on a linear basis. Both analyses yield the same optimal heuristic I&M strategy. Finally, to determine the cost-effectiveness of the identified optimal I&M strategy, a DV analysis is carried out considering the probabilistic I&M cost model.

Based on our work, the following conclusions can be drawn.

1. The generic framework described in Sect. 2 facilitates an optimization of I&M regimes for turbine support structures in offshore wind farms taking into account the uncertainties in the I&M costs.

2. The proposed probabilistic cost model can be utilized to quantify I&M costs at wind farm, structural system, and component level, which can be updated when new data on the parameters governing the I&M costs become available during the operation of wind farms.

3. The sensitivity analyses showed that, at component level, the campaign cost and engineering cost have the highest influence on the overall I&M cost, while the vessel cost per shift has the highest impact on the overall I&M costs at structural system and wind farm level.

4. The decision analysis described in the numerical example identifies a cost and risk optimal I&M strategy for a steel frame subject to fatigue based on the probabilistic cost model. An optimal inspection interval of $\Delta t = 8$ years is obtained from the PIPA-DA and DV analysis. Furthermore, if the annual system failure probability exceeds a threshold of $p_{\text{th}} = 1 \times 10^{-3}$ yr^{-1}, an additional inspection campaign is launched. In each campaign, six prioritized hotspots are inspected, and a repair campaign is launched if fatigue cracks are indicated and measured to be deeper than $a_R = 1$ mm.

Table 7. Cost model normalized with respect to the expected campaign cost.

Cost parameter	Ratio	Normalized value
Campaign cost c_C	$9.11 \times 10^3 / 9.11 \times 10^3$	1.00
Failure cost c_F	$2.00 \times 10^7 / 9.11 \times 10^3$	2193.77
Engineering cost c_E	$4.55 \times 10^4 / 9.11 \times 10^3$	5.00
Inspection cost below water with EM $c_{I,Op}$	$8.87 \times 10^3 / 9.11 \times 10^3$	0.97
Inspection cost above water with EM $c_{I,Op}$	$3.54 \times 10^3 / 9.11 \times 10^3$	0.38
Repair cost below water with welding $c_{M,Op}$	$4.58 \times 10^4 / 9.11 \times 10^3$	5.02
Repair cost above water with welding $c_{M,Op}$	$3.80 \times 10^4 / 9.11 \times 10^3$	4.17

Table 8. Cost model normalized with respect to the failure cost.

Cost parameter	Ratio	Normalized value
Failure cost c_F	$2.00 \times 10^7 / 2.00 \times 10^7$	1.0
Campaign cost c_C	$9.11 \times 10^3 / 2.00 \times 10^7$	4.55×10^{-4}
Engineering cost c_E	$4.55 \times 10^4 / 2.00 \times 10^7$	2.28×10^{-3}
Inspection cost below water with EM $c_{I,Op}$	$8.87 \times 10^3 / 2.00 \times 10^7$	4.43×10^{-4}
Inspection cost above water with EM $c_{I,Op}$	$3.54 \times 10^3 / 2.00 \times 10^7$	1.77×10^{-4}
Repair cost below water with welding $c_{M,Op}$	$4.58 \times 10^4 / 2.00 \times 10^7$	2.29×10^{-3}
Repair cost above water with welding $c_{M,Op}$	$3.80 \times 10^4 / 2.00 \times 10^7$	1.90×10^{-3}

5. With the help of the numerical example, it is demonstrated that the I&M costs can be considered deterministically as expected values in the decision analysis if they are included in the optimization on a linear basis.

6. The expected I&M costs at the structural system level depend solely on the number of campaigns and components involved in the I&M operations as well as on the expected campaign, engineering, and operational cost, which therefore can be normalized and used in decision analyses to optimize the I&M regime of support structures at the structural system level. In the future, we will research similar concepts to derive deterministic (normalized) cost models for I&M planning at wind farm level.

Appendix A: Expected utilities and optimal I&M decisions

As described in Sect. 2.1, the expected utilities $\mathbb{E}[U_0]$, $\mathbb{E}[U_1|\boldsymbol{a}]$, and $\mathbb{E}[U_2|i]$ form the basis for utility-informed optimizations of inspection and monitoring as well as maintenance of WT support structures in offshore wind farms. This Appendix briefly summarizes the evaluation of these expected utilities. The summary assumes that the corresponding utility functions and the probability distributions of their input parameters are available. In addition, the Appendix shows in more detail how decisions on inspection and monitoring as well as maintenance are optimized by maximizing the corresponding expected utilities.

A1 System state analysis

As part of the system state analysis (SS-A), the expected utility $\mathbb{E}[U_0]$ is evaluated as follows:

$$\mathbb{E}[U_0] = E_{X,W}[U_0(X,W)]$$
$$= \int_X \int_W U_0(\boldsymbol{x},\boldsymbol{w})\, p(\boldsymbol{x},\boldsymbol{w})\, \mathrm{d}\boldsymbol{w}\, \mathrm{d}\boldsymbol{x}, \tag{A1}$$

where $\mathbb{E}_{X,W}[U_0(X,W)]$ is the expected value of the utility function $U_0(\boldsymbol{X},\boldsymbol{W})$ defined in Eq. (1) with respect to random variables $\boldsymbol{X}$ and $\boldsymbol{W}$, which influence the system state and the I&M costs, and $p(\boldsymbol{x},\boldsymbol{w})$ is the joint prior probability distribution of $\boldsymbol{X}$ and $\boldsymbol{W}$.

A2 Predicted action decision analysis

In the predicted action decision analysis (PA-DA), the expected utility $\mathbb{E}[U_1|\boldsymbol{a}]$ is evaluated. This expected utility is conditional on a possible choice of maintenance actions $\boldsymbol{a}$ and computed with respect to the random variables $\boldsymbol{Y}$, $\boldsymbol{X}$, and $\boldsymbol{W}$. These random variables influence the outcome of the associated maintenance actions, the system state, and the I&M costs. In a generic format, $\mathbb{E}[U_1|\boldsymbol{a}]$ is determined as

$$\mathbb{E}[U_1|\boldsymbol{a}] = \mathbb{E}_{Y,X,W}[U_1(\boldsymbol{a},Y,X,W)]$$
$$= \int_Y \int_X \int_W U_1(\boldsymbol{a},\boldsymbol{y},\boldsymbol{x},\boldsymbol{w})\, p(\boldsymbol{y},\boldsymbol{x},\boldsymbol{w})\, \mathrm{d}\boldsymbol{w}\, \mathrm{d}\boldsymbol{x}\, \mathrm{d}\boldsymbol{y}, \tag{A2}$$

where $\mathbb{E}_{Y,X,W}[U_1(\boldsymbol{a},Y,X,W)]$ is the expected value of the utility function $U_1(\boldsymbol{a},\boldsymbol{Y},\boldsymbol{X},\boldsymbol{W})$ defined in Eq. (2) with re-

spect to Y, X, and W, and $p(y, x, w)$ is the joint prior probability distribution of Y, X, and W.

The optimal maintenance actions a^* are identified by maximizing the conditional expected value of U_1 as

$$a^* = \arg\max_a \mathbb{E}[U_1|a]. \tag{A3}$$

Finally, the expected value of U_1 conditional on the optimal maintenance actions a^* can be defined as

$$\mathbb{E}[U_1|a^*] = \mathbb{E}_{Y,X,W}[U_1(a^*, Y, X, W)]. \tag{A4}$$

A3 Predicted information and predicted action decision analysis

A predicted information and predicted action decision analysis (PIPA-DA) is performed to jointly optimize decisions on inspection and monitoring as well as maintenance (see also Thöns and Kapoor, 2019). In this analysis, the expected value of the utility U_2 is maximized based on predicted inspection and monitoring outcomes and predicted maintenance actions. When applying the extensive form of the analysis based on the lower branch of the decision tree in Fig. 1 (Raiffa and Schlaifer, 1961), the optimization is progressed from the leaf of the branch towards the node representing the decision on the inspection and monitoring regime i. The analysis starts by determining the expected value of U_2 conditional on a choice of the inspection and monitoring regime i, a realization of the corresponding inspection and monitoring outcomes $Z_i = z_i$, and a possible choice of maintenance actions a as follows:

$$\mathbb{E}[U_2|i, z_i, a] = \mathbb{E}_{Y,X,W|Z_i=z_i}[U_2(i, z_i, a, Y, X, W)]$$
$$= \int_Y \int_X \int_W U_2(i, z_i, a, Y, X, W) \, p(y, x, w|z_i) \, dw \, dx \, dy. \tag{A5}$$

where $\mathbb{E}_{Y,X,W|Z_i=z_i}[U_2(i, z_i, a, Y, X, W)]$ is the conditional expected value of the utility function $U_2(i, z_i, a, Y, X, W)$ defined in Eq. (3) with respect to Y, X, and W conditional on $Z_i = z_i$, and $p(y, x, w|z_i)$ is the joint posterior probability distribution of Y, X, and W given $Z_i = z_i$, which is determined using Bayesian analysis.

Subsequently, the optimal maintenance actions $a^*_{|i, z_i}$ conditional on a certain choice of the inspection and monitoring regime i and a corresponding realization of the inspection and monitoring outcomes $Z_i = z_i$ can be determined by maximizing $\mathbb{E}[U_2|i, z_i, a]$ as

$$a^*_{|i, z_i} = \arg\max_a \mathbb{E}[U_2|i, z_i, a]. \tag{A6}$$

Given that the decision-maker upon knowing the inspection and monitoring outcomes $Z_i = z_i$ will always make the optimal maintenance decisions $a^*_{|i, z_i}$, the expected value of the utility U_2 conditional on a choice of the inspection and

monitoring regime i is computed as

$$\mathbb{E}[U_2|i] = \mathbb{E}_{Z_i}[\mathbb{E}_{Y,X,W|Z_i}[U_2(i, Z_i, a^*_{|i, Z_i}, Y, X, W)]]$$
$$= \int_{Z_i} [\max_a \mathbb{E}_{Y,X,W|Z_i=z_i}[U_2(i, z_i, a, Y, X, W)]] \, p(z_i) dz_i, \tag{A7}$$

where $\mathbb{E}_{Z_i}[\cdot]$ is the expectation with respect to Z_i, and $p(z_i)$ is the marginal probability distribution of the probabilistic inspection and monitoring outcomes Z_i. The optimal inspection and maintenance regime i^* is then obtained by maximizing $\mathbb{E}[U_2|i]$ as

$$i^* = \arg\max_i \mathbb{E}[U_2|i]. \tag{A8}$$

Finally, the maximum expected value of U_2 conditional on i^* is obtained as

$$\mathbb{E}[U_2|i^*]$$
$$= \mathbb{E}_{Z_{i^*}}[\mathbb{E}_{Y,X,W|Z_{i^*}}[U_2(i^*, Z_{i^*}, a^*_{|i^*, Z_{i^*}}, Y, X, W)]]. \tag{A9}$$

From Eqs. (A6), (A7), and (A8) it can be seen that a PIPA-DA cannot be summarized in a single optimization problem if the extensive form of the analysis is applied. As shown in Eq. (A6), the optimal decisions on the maintenance actions $a^*_{|i, z_i}$ can in this case only be determined conditional on a certain realization of the inspection and monitoring outcomes $Z_i = z_i$.

Appendix B: Expected total lifetime cost conditional on a heuristic I&M strategy

The expected value of the total lifetime cost $\mathbb{E}[C_2|\mathcal{S}_\theta]$ conditional on a heuristic I&M strategy $\mathcal{S}_\theta$ is required to identify the cost- and risk-informed optimal heuristic I&M strategy $\mathcal{S}_{\theta^*}$ as described in the numerical example in Sect. 6. In the following, we outline the evaluation of $\mathbb{E}[C_2|\mathcal{S}_\theta]$ considering probabilistic and expected I&M costs.

B1 Probabilistic I&M costs

The expected total lifetime cost $\mathbb{E}[C_2|\mathcal{S}_\theta]$ considering probabilistic I&M costs is defined as

$$\mathbb{E}[C_2|\mathcal{S}_\theta] = E_{X,Y,Z,W}[C_2(\mathcal{S}_\theta, X, Y, Z, W)]$$
$$= \int_X \int_Y \int_Z \int_W C_2(\mathcal{S}_\theta, X, Y, Z, W) \, p(x, y, z|\mathcal{S}_\theta)$$
$$p(w|\mathcal{S}_\theta) \, dx \, dy \, dz \, dw, \tag{B1}$$

in which $p(x, y, z|\mathcal{S}_\theta) \, p(w|\mathcal{S}_\theta)$ is the joint probability density function (PDF) of X, Y, Z, and W. Equation (B1) implies that the uncertain parameters W governing the I&M costs are modeled as statistically independent of the uncertain parameters X influencing the system failure probability, the uncertain parameters Y affecting the repair outcomes, and the probabilistic inspection outcomes Z.

Equation (B1) can be rewritten as

$$\mathbb{E}[C_2|\mathcal{S}_\theta] = \int_Z \int_W \mathbb{E}[C_2|\mathcal{S}_\theta, z, \boldsymbol{w}] \, p(z|\mathcal{S}_\theta) \, p(\boldsymbol{w}|\mathcal{S}_\theta) \mathrm{d}z \, \mathrm{d}\boldsymbol{w}, \quad \text{(B2)}$$

where $\mathbb{E}[C_2|\mathcal{S}_\theta, z, \boldsymbol{w}]$ is the expected total lifetime cost conditional on the inspection outcomes $\boldsymbol{Z} = z$, and corresponding repairs as prescribed by strategy $\mathcal{S}_\theta$ and $p(z|\mathcal{S}_\theta)$ represent the marginal PDF of the lifetime inspection outcomes.

$\mathbb{E}[C_2|\mathcal{S}_\theta, z, \boldsymbol{w}]$ is computed as

$$\mathbb{E}[C_2|\mathcal{S}_\theta, z, \boldsymbol{w}] = \mathbb{E}_{X, Y|Z=z, W=w}[C_2(\mathcal{S}_\theta, X, Y, z, \boldsymbol{w})]$$

$$= \int_X \int_Y C_2(\mathcal{S}_\theta, X, Y, z, \boldsymbol{w}) \, p(\boldsymbol{x}, \boldsymbol{y}|\mathcal{S}_\theta, z) \, \mathrm{d}\boldsymbol{x} \, \mathrm{d}\boldsymbol{y}, \quad \text{(B3)}$$

where $p(\boldsymbol{x}, \boldsymbol{y}|\mathcal{S}_\theta, z)$ is the conditional PDF of X and Y given $\boldsymbol{Z} = z$. $\mathbb{E}[C_2|\mathcal{S}_\theta, z, \boldsymbol{w}]$ can be decomposed as

$$\mathbb{E}[C_2|\mathcal{S}_\theta, z, \boldsymbol{w}] = \mathbb{E}[C_I|\mathcal{S}_\theta, z, \boldsymbol{w}] + \mathbb{E}[C_M|\mathcal{S}_\theta, z, \boldsymbol{w}]$$

$$+ \mathbb{E}[C_F|\mathcal{S}_\theta, z], \quad \text{(B4)}$$

where $\mathbb{E}[C_I|\mathcal{S}_\theta, z, \boldsymbol{w}]$ is the conditional expected lifetime inspection cost, $\mathbb{E}[C_M|\mathcal{S}_\theta, z, \boldsymbol{w}]$ is the conditional expected lifetime maintenance cost, and $\mathbb{E}[C_F|\mathcal{S}_\theta, z]$ quantifies the conditional expected lifetime failure costs over the lifetime of the structure. Note that the latter does not depend on the I&M cost model parameters as shown in Eq. (B7) below.

The conditional expected lifetime inspection cost $\mathbb{E}[C_I|\mathcal{S}, z, \boldsymbol{w}]$ is computed as

$$\mathbb{E}[C_I|\mathcal{S}_\theta, z, \boldsymbol{w}] = \sum_{j=1}^{m} C_{I,j}(\mathcal{S}_\theta, z, \boldsymbol{w})$$

$$\cdot \gamma_j \cdot [1 - \Pr(F_j|\mathcal{S}_\theta, z)], \quad \text{(B5)}$$

where the jth term represents the inspection costs in year j given that failure has not occurred up to the end of that year; $C_{I,j}(\mathcal{S}_\theta, z, \boldsymbol{w})$ is the inspection cost in year j, which is estimated based on the model defined in Eq. (11); and $1 - \Pr(F_j|\mathcal{S}_\theta, z)$ is the probability of survival of the system up to the end of year j conditional on the inspection outcomes $\boldsymbol{Z} = z$ and corresponding repairs as determined by the strategy S.

Similarly, the conditional expected lifetime maintenance cost $\mathbb{E}[C_M|\mathcal{S}_\theta, z, \boldsymbol{w}]$ is given by

$$\mathbb{E}[C_M|\mathcal{S}_\theta, z, \boldsymbol{w}] = \sum_{j=1}^{m} C_{M,j}(\mathcal{S}_\theta, z, \boldsymbol{w}) \cdot \gamma_j$$

$$\cdot [1 - \Pr(F_j|\mathcal{S}_\theta, z)], \quad \text{(B6)}$$

where $C_{M,j}(\mathcal{S}_\theta, z, \boldsymbol{w})$ is the maintenance cost in year j, which is determined based on the model defined in Eq. (12).

The conditional expected lifetime failure cost $\mathbb{E}[C_F|\mathcal{S}_\theta, z, \boldsymbol{w}]$ is evaluated as

$$\mathbb{E}[C_F|\mathcal{S}_\theta, z] = \sum_{j=1}^{m} c_F \cdot \gamma_j \cdot [\Pr(F_j|\mathcal{S}_\theta, z) - \Pr(F_{j-1}|\mathcal{S}_\theta, z)], \quad \text{(B7)}$$

where c_F is the deterministic failure cost and $\Pr(F_j|\mathcal{S}_\theta, z) - \Pr(F_{j-1}|\mathcal{S}_\theta, z)$ is the probability of failure for year j given $\boldsymbol{Z} = z$ (see also Eq. 15).

$\mathbb{E}[C_2|\mathcal{S}_\theta]$ is estimated here using an MC approach:

$$\mathbb{E}[C_2|\mathcal{S}_\theta] =$$

$$\int_Z \int_W \mathbb{E}[C_2|\mathcal{S}_\theta, z, \boldsymbol{w}] \, p(z|\mathcal{S}_\theta) \, p(\boldsymbol{w}|\mathcal{S}_\theta) \mathrm{d}z \, \mathrm{d}\boldsymbol{w}$$

$$\approx \frac{1}{n} \sum_{i=1}^{n} \mathbb{E}\left[C_2|\mathcal{S}_\theta, z^{(i)}, \boldsymbol{w}^{(i)}\right], \quad \text{(B8)}$$

in which $\{z^{(i)}\}_{i=1}^{n}$ represents samples of the probabilistic inspection outcomes $\boldsymbol{Z}$ conditional on the heuristic strategy $\mathcal{S}_\theta$, which are generated as discussed by Bismut and Straub (2021); $\{\boldsymbol{w}^{(i)}\}_{i=1}^{n}$ represents samples of the uncertain cost model parameters $\boldsymbol{W} = [W_1^T, \ldots, W_m^T]^T$, where W_j represents the probabilistic parameters influencing the I&M costs in year j as defined in Table 5. As described in Sect. 6.2, it is assumed that the different W_j, $j = 1, \ldots, m$ values are independent and identically distributed. Thus, the joint PDF $p(\boldsymbol{w}|\mathcal{S}_\theta)$ can simply be written as $p(\boldsymbol{w}|\mathcal{S}_\theta) = p(\boldsymbol{w}_1|\mathcal{S}_\theta) \cdot \ldots \cdot p(\boldsymbol{w}_m|\mathcal{S}_\theta)$. It is further assumed that repair solutions are pre-engineered before the frame is commissioned. Thus, the engineering costs are only incurred once at the beginning of the lifetime.

The expected lifetime cost $\mathbb{E}[C_2|\mathcal{S}_\theta]$ is in this contribution estimated using MCS with 400 samples of the inspection outcome $\boldsymbol{Z}$ and cost model parameters $\boldsymbol{W}$.

B2 Expected I&M costs

Based on Eq. (19), the conditional expected lifetime inspection cost can be formulated such that it only depends on the inspection outcomes $\boldsymbol{Z} = z$ and corresponding repairs as determined by the strategy $\mathcal{S}_\theta$, i.e.,

$$\mathbb{E}[C_I|\mathcal{S}_\theta, z] = \mathbb{E}_{W|Z=z}[C_I|\mathcal{S}_\theta, z, \boldsymbol{W}]$$

$$= \sum_{j=1}^{m} \mathbb{E}_{W|Z=z}[C_{I,j}(\mathcal{S}_\theta, z, \boldsymbol{W})] \cdot \gamma_j \cdot [1 - \Pr(F_j|\mathcal{S}_\theta, z)] \quad \text{(B9)}$$

with

$$\mathbb{E}_{W|Z=z}[C_{I,j}(\mathcal{S}_\theta, z, \boldsymbol{W})] = n_{C,j}(\mathcal{S}_\theta, z) \cdot \mathbb{E}[C_C]$$

$$+ n_{I,C,j}(\mathcal{S}_\theta, z) \cdot \mathbb{E}[C_{I,Op}], \quad \text{(B10)}$$

where $n_{C,j}(\mathcal{S}_\theta, z)$ and $n_{I,C,j}(\mathcal{S}_\theta, z)$ are the total numbers of inspection campaigns and component inspections in year j.

Equivalently, based on Eq. (20), the conditional expected lifetime maintenance cost can be expressed as

$$\mathbb{E}[C_M|\mathcal{S}_\theta, z] = \mathbb{E}_{W|Z=z}[C_M|\mathcal{S}_\theta, z, \boldsymbol{W}] =$$

$$\sum_{j=1}^{m} \mathbb{E}_{W|Z=z}[C_{M,j}(\mathcal{S}_\theta, z, \boldsymbol{W})] \cdot \gamma_j \cdot [1 - \Pr(F_j|\mathcal{S}_\theta, z)] \quad \text{(B11)}$$

with

$$\mathbb{E}_{W|Z=z}\big[c_{M,j}\big(\mathcal{S}_\theta, z, W\big)\big] = n_{C,j}\big(\mathcal{S}_\theta, z\big) \cdot \big(\mathbb{E}\big[C_C\big]$$
$$+ \mathbb{E}\big[C_E\big]\big) + n_{M,C,j}\big(\mathcal{S}_\theta, z\big) \cdot E\big[C_{M,Op}\big], \qquad (B12)$$

where $n_{C,j}(\mathcal{S}_\theta, z)$ and $n_{M,C,j}(\mathcal{S}_\theta, z)$ are the number of repair campaigns and component repairs in year j. Note that the models defined in Eqs. (B10) and (B12) do not explicitly account for the inspection and repair location or methods to simplify the notation.

Based on Eqs. (B7), (B9), and (B11), the expected total lifetime cost can now be written to depend only on the heuristic I&M strategy $\mathcal{S}_\theta$ and the inspection outcomes $Z = z$:

$$\mathbb{E}[C_2|\mathcal{S}_\theta, z] = \mathbb{E}[C_I|\mathcal{S}_\theta, z] + \mathbb{E}[C_M|\mathcal{S}_\theta, z] + \mathbb{E}[C_F|\mathcal{S}_\theta, z]. \quad (B13)$$

After evaluating the expected total lifetime cost conditional on the inspection outcomes $Z = z$, $\mathbb{E}[C_2|\mathcal{S}_\theta]$ can be computed as

$$\mathbb{E}[C_2|\mathcal{S}_\theta] = \int_Z \mathbb{E}[C_2|\mathcal{S}_\theta, \mathbf{z}] \, p(z|\mathcal{S}_\theta) \mathrm{d}z. \qquad (B14)$$

The integral in Eq. (B14) can be solved using an MC approach similar to Eq. (B8).

Code availability. The code used in this study is not publicly available. However, relevant details underlying the implementation are described in the paper and referenced works (Schneider et al., 2017; Schneider, 2020; Eichner et al., 2023).

Data availability. The data required for building the models are provided in Tables 1–5 (cost modeling and sensitivity study) and Sect. 6 of the publication, along with the model data summarized in Eichner et al. (2023) for the numerical example. No additional datasets were generated or analyzed during this study.

Author contributions. MF: conceptualization, methodology, software, formal analysis, data curation, validation, writing (original draft). RS: conceptualization, methodology, software, formal analysis, data curation, validation, supervision, writing (review and editing). ST: funding acquisition, supervision, conceptualization, methodology, writing (review and editing). MG: supervision, writing (review and editing).

Competing interests. The contact author has declared that none of the authors has any competing interests.

Disclaimer. Publisher's note: Copernicus Publications remains neutral with regard to jurisdictional claims made in the text, published maps, institutional affiliations, or any other geographical representation in this paper. While Copernicus Publications makes every effort to include appropriate place names, the final responsibility lies with the authors.

References

Bismut, E. and Straub, D.: Optimal adaptive inspection and maintenance planning for deteriorating structural systems, Reliab. Eng. Syst. Safe, 215, 107891, https://doi.org/10.1016/j.ress.2021.107891, 2021.

Bismut, E., Luque, J., and Straub, D.: Optimal prioritization of inspections in structural systems considering component interactions and interdependence, 12th International Conference on Structural Safety & Reliability (ICOSSAR 2017), 6–10 August 2017, Vienna, Austria, 2017.

Eichner, L., Schneider, R., and Baeßler, M.: Optimal vibration sensor placement for jacket support structures of offshore wind turbines based on value of information analysis, Ocean Eng., 288, 115407, https://doi.org/10.1016/j.oceaneng.2023.115407, 2023.

Farhan, M., Schneider, R., and Thöns, S.: Predictive information and maintenance optimization based on decision theory: A case study considering a welded joint in an offshore wind turbine support structure, Struct. Health Monit., 21, 185–207, https://doi.org/10.1177/1475921720981833, 2021.

Florian, M. and Sorensen, J. D.: Risk-based planning of operation and maintenance for offshore wind farms, Enrgy Proced., 137, 261–272, https://doi.org/10.1016/j.egypro.2017.10.349, 2017.

Luque, J. and Straub, D.: Risk-based optimal inspection strategies for structural systems using dynamic Bayesian networks, Struct. Saf., 76, 68–80, https://doi.org/10.1016/j.strusafe.2018.08.002, 2019.

Martinez-Luengo, M. and Shafiee, M.: Guidelines and Cost-Benefit Analysis of the Struct. Health Monit. Implementation in Offshore Wind Turbine Support Structures, Energies, 12, 1176, https://doi.org/10.3390/en12061176, 2019.

Morato, P. G., Andriotis, C. P., Papakonstantinou, K. G., and Rigo, P.: Inference and dynamic decision-making for deteriorating systems with probabilistic dependencies through Bayesian networks and deep reinforcement learning, Reliab. Eng. Syst. Safe, 235, 109144, https://doi.org/10.1016/j.ress.2023.109144, 2023.

Moy, R., Chen, L., and Kao, L.: Normal and Lognormal Distributions, in: Study Guide for Statistics for Business and Financial Economics: A Supplement to the Textbook by Cheng-Few Lee, John C. Lee and Alice C. Lee, edited by: Moy, R. L., Chen, L.-S., and Kao, L. J., Springer International Publishing, Cham, 83–97, https://doi.org/10.1007/978-3-319-11997-7_7, 2015.

Nielsen, J. S. and Sorensen, J. D.: On risk-based operation and maintenance of offshore wind turbine components, Reliab. Eng. Syst. Safe, 96, 218–229, https://doi.org/10.1016/j.ress.2010.07.007, 2011.

Nielsen, J. S. and Sorensen, J. D.: Risk-based derivation of target reliability levels for life extension of wind turbine structural components, Wind Energy, 24, 939–956, https://doi.org/10.1002/we.2610, 2021.

Raiffa, H. and Schlaifer, R.: Applied Statistical Decision Theory, Clinton Press, Inc, Boston, ISBN 978-0-471-38349-9, 1961.

Rodriguez-Sanchez, J. E., Dover, W. D., and Brennan, F. P.: Application of short repairs for fatigue life extension, Int. J. Fatigue, 26, 413–420, https://doi.org/10.1016/j.ijfatigue.2003.07.002, 2004.

Rodriguez-Sanchez, J. E., Rodriguez-Castellanos, A., Perez-Guerrero, F., Carbajal-Romero, M. F., and Liu, S.: Offshore fatigue crack repair by grinding and wet welding, Fatigue Fract. Eng. M., 34, 487–497, https://doi.org/10.1111/j.1460-2695.2010.01541.x, 2011.

Schneider, R.: Effect of repair models on risk-based optimal inspection strategies for support structures of offshore wind turbines, SMAR - Fifth Conference on Smart Monitoring, Assessment and Rehabilitation of Civil Structures, Berlin-Potsdam, 27–29 August 2019.

Schneider, R.: Time-variant reliability of deteriorating structural systems conditional on inspection and monitoring data, Ingenieurfakultät Bau Geo Umwelt, Technische Universität München, München, 1–188 pp., ISBN 1613-4249, 2020.

Schneider, R., Thöns, S., and Straub, D.: Reliability analysis and updating of deteriorating systems with subset simulation, Struct. Saf., 64, 20–36, https://doi.org/10.1016/j.strusafe.2016.09.002, 2017.

Schneider, R., Rogge, A., Thöns, S., Bismut, E., and Straub, D.: A sampling-based approach to identifying optimal inspection and repair strategies for offshore jacket structures, Life-Cycle Analysis and Assessment in Civil Engineering: Towards an Integrated Vision, Ghent, Belgium, 2018.

Sobol, I. M.: On sensitivity estimation for nonlinear mathematical models, Mathematical Modelling and Computational Experiment 1, 407–414, 1993.

Sobol, I. M.: Global sensitivity indices for nonlinear mathematical models and their Monte Carlo estimates, Math. Comput. Simulat., 55, 271–280, https://doi.org/10.1016/S0378-4754(00)00270-6, 2001.

Sorensen, J. D.: Framework for Risk-based Planning of Operation and Maintenance for Offshore Wind Turbines, Wind Energy, 12, 493–506, https://doi.org/10.1002/we.344, 2009.

Straub, D.: Generic approaches to risk based inspection planning for steel structures, PhD Thesis, Swiss Federal Institute of Technology Zurich, Institute of Structural Engineering, 248 pp., https://doi.org/10.3929/ethz-a-004783633, 2004.

Straub, D. and Faber, M. H.: System Effects in Generic Risk-Based Inspection Planning, J. Offshore Mech. Arct. Eng., 126, 265–271, https://doi.org/10.1115/1.1782642, 2004.

Thöns, S.: On the Value of Monitoring Information for the Structural Integrity and Risk Management, Comput-Aided Civ. Inf., 33, 79–94, https://doi.org/10.1111/mice.12332, 2018.

Thöns, S. and Kapoor, M.: Value of information and value of decisions, ICASP13, Seoul, South Korea, 26–30 May 2019.

Thöns, S., Faber, M. H., and Val, D.: On the Value of Structural Health Monitoring Information for the Operation of Wind Parks, ICOSSAR 2017, Vienna, Austria, 2017.

Von Neumann, J. and Morgenstern, O.: Theory of games and economic behavior, Princeton University Press, Princeton, ISBN 978-0691130613 (60th anniversary edition), 1947.